Cylindrical Reflector SKA

Authors:
John D. Bunton CSIRO Telecommunications and Industrial Physics
Carole A. Jackson RSAA, Australian National University
Elaine M. Sadler School of Physics, University of Sydney

Submitted to the SKA Engineering and Management Team by

The Executive Secretary
Australian SKA Consortium Committee
PO Box 76, Epping, NSW 1710, Australia
June 2002

Updated 11 July 2002

Table of contents

Executive summary

One key to a cost effective SKA, at frequencies above one GigaHertz, is a low-cost reflector or lens. Historical comparisons show that the elimination of one axis of rotation and one degree of curvature of the surface can reduce the cost of cylindrical reflectors by a factor of six when compared to comparable parabolic dish reflectors. However, the feed structure for a cylindrical reflector is costlier, reducing this advantage somewhat. The cylindrical antenna is in effect a marriage between reflector and phased array technology -- focusing is due to the reflector in one direction, while in the orthogonal direction it is due to phasing and beamforming of the feed structure.

A cylindrical reflector has some of the advantages of both reflector and phased-array technologies. It provides another degree of freedom compared to pure reflector solutions while still minimising costs. This extra degree of freedom allows a field-of-view of up to 200 square degrees at 1.4 GHz, which is about two orders of magnitude greater than parabolic dishes. Compared to the phased array, the loss of one degree of freedom reduces the field-of-view by the same amount. This reduces the cost of feeds and beamformers by a large factor when compared to a phased array. This allows a cylindrical reflector based SKA to operate at much higher frequencies than would be possible with a phased array based SKA.

In this proposal, we envisage a maximum initial operating frequency of 9GHz using 15m by 111m antennas, with the possibility of future upgrades reaching 20-24GHz at reduced sensitivity. The wide reflector sets the lowest operating frequency at 100 MHz, providing an instrument that is a sensitive probe into the Early Universe.

High dynamic range is achieved by configuring the antenna as eight separate contiguous units, each of which provides a one-degree beam at 1.4GHz. With an SKA made of 600 antennas a 4800 input correlator is needed. The large number of inputs result in a snapshot dynamic range of ~100,000:1. Multi-frequency synthesis and longer integration times will increase the dynamic range to well over a million to one. For high-speed survey work, the full line feed of each antenna can be beamformed to generate fan beams. The correlator, without any increase in size, can process the 64 fan beams generated in this way, and image eight square degrees in a single snapshot.

To keep within cost constraints, the instantaneously accessible sky is limited to 8 one-square-degree beams lying in a 40 by 1 degree area of the sky at 1.4GHz. For each frequency band that the line feed array covers, a separate pointing is allowed within a 120-degree arc. For the antennas within 10 km of the central core of the array, the signal for all eight beams is brought to the correlator. As distance increases the number is progressively reduced so that at 3000km only a single one-degree beam is processed, again this reduction is necessary to contain costs. The array design itself follows the principle of equal effective area at baseline scales from 1 to 10,000km. For baselines scaling by a factor of three, the resulting effective area at each baseline is 0.47 of the total area. The cost of this concept in current dollars is estimated at: **Cost of SKA = 549 + 90*BW + 9.6*BW*b US$M** where BW is the bandwidth processed and b is the number of one degree beams. Thus, a 2.4GHz-bandwidth instrument with up to 8 one-degree beams operating at up to 9GHz is about one billion US dollars (2002 prices).

1 Introduction

It is almost universally accepted that two-dimensional phased arrays, such as LOFAR Bregman [1.1], are the optimum technology at low frequencies. At high frequencies, such as those covered by ALMA, fully steerable parabolic reflectors are used. The SKA will observe at frequencies in between these: 100 MHz to 20 GHz. In this range of frequencies, there is no ready consensus as to the best technology. The number of feed elements in two-dimensional phased arrays grows quadratically with frequency. In comparison, the field-of-view of a parabolic reflector diminishes quadratically with frequency. Moreover, reflectors are not cost effective at low frequencies especially if designed with the precision needed at high frequencies. It is unlikely that any single technology can cover the possibly 200:1 or greater frequency range of the SKA and provide the lowest cost solution at all frequencies. Inevitably, there will be some frequency range where an alternative technology would have provided a cheaper solution. Thus, the final SKA implementations will be a complex optimisation in which the trade-off between planar arrays and steerable dishes is potentially a central issue.

This leads to the consideration of cylindrical reflectors[1] that exploit the best of the technologies that are optimum at the extremes of the SKA frequency range. Using reflector technology to form the beam in one direction and phased array technology for the orthogonal direction. The field-of-view is restricted when compared to a phased array, but is larger than that of a parabolic reflector. At 1.4GHz the instantaneous field-of-view of a small parabolic reflector for the SKA is 1 to 4 square degrees. For a cylindrical reflector it can be two orders of magnitude greater: 120 to 240 square degrees. A phased array would be two orders of magnitude greater still, at about 10,000 square degrees. Cylindrical reflectors fall mid-way between parabolic reflectors and phased arrays in terms of field-of-view.

The cylindrical reflector provides an antenna with enhanced multibeaming capabilities when compared to a parabolic reflector and is economical at frequencies much higher than those practical for a phased array. The proposed design is for a cylindrical reflector of width 15m with a surface good to 12GHz. The initial line feed would set the upper frequency limit to 9GHz. Upgrades to 12GHz and beyond would be attractive especially if future developments provide low-noise uncooled LNAs at these frequencies. Aperture efficiency beyond 12 GHz will be lower, but operation at frequencies as high as 24GHz may nonetheless be possible.

With cylindrical reflectors, antenna stations can be built as a single long reflector. This is no costlier than multiple reflectors and allows the beam area to be maximised for a given antenna station effective area. Maximising the beam area reduces the number of beams needed to image a given area and this results in reduced signal transport and correlator costs.

[1] For brevity cylindrical antenna or reflector will refer to an antenna or reflector whose surface is in the form of a cylindrical paraboloid.

1.1 Relative Costs: the best of both worlds

The cost of a planar phased array is driven by the number of elements, which is proportional to the square of the maximum operating frequency. For the line feed of a cylindrical reflector the technology is similar but the costs scale directly with frequency. Thus when compared to a phased array SKA the line feed costs of a cylindrical reflector are small. The cost of the reflector must then be added to this.

The reflector component of a cylindrical antenna is less costly than a parabolic reflector. An estimate of the cost reduction can be found by comparing the cost of existing radio telescopes. For antennas of similar dimensions and maximum frequency, a Molonglo-style cylindrical reflector is six times cheaper per unit area than one which uses the technology adopted in the Lovell, Parkes, Effelsberg or GBT reflectors (see Appendix A for details of this calculation). This arises because one axis of rotation is eliminated, construction takes place at or near ground level and the surface is curved in only one direction. For the SKA, we estimate that cylindrical reflectors based on Molonglo construction techniques would cost about US$300M, excluding site acquisition, with a surface that is good for frequencies up to 12GHz. The line feed, uncooled LNAs and initial RF beamformers will approximate double this cost.

As cylindrical reflectors have not been popular for the last 35 years, some have considered it not to be a viable technology. The historical reasons behind this are explored in [Appendix B]. In summary, it is found that beamforming was a major problem that resulted in narrow band systems with high system noise and limited upgradeabilty. But in the SKA beamforming is a problem for most designs. Advances in digital beamforming overcome this problem. This, together with broadband line feeds and high-performance uncooled LNAs, make cylindrical reflectors an increasingly viable option. In the sense that it can provide a wide field-of-view at frequencies up to 10GHz and beyond, it is not only viable but a close to optimal solution to the SKA problem over the 1 to 10GHz frequency range.

The major challenge in achieving this goal is the design of line feeds to illuminate the reflector. The line feed can be thought of a one-dimensional phased array and it will be difficult to achieve very wide bandwidths. To cover the required frequency range a number of scaled line feeds will be needed each covering at least a 2:1 frequency range. This will be a major challenge in terms of achieving the required bandwidth, polarisation purity, calibration, noise performance and fabrication cost. Associated with the line feed is the challenge of developing suitable downconverters and digitisers. Here radio-on-a-chip concepts are the way forward.

1.2 Instrument Overview

The SKA implementation proposed here consists of 600 antenna stations, each comprising a single 15m x 111m cylindrical reflector, illustrated below, operating over the frequency range 100MHz to 9GHz. The East-West horizontal axis reflector has the advantage of full declination coverage at transit even though the sky coverage is limited to about 70% of the visible sky. It is proposed that the array configurations cover baselines of 1, 3, 10, 30, 100, 300, 1000, 3000 and 10,000 km. For the whole array the

Aeff/Tsys is 2×10^4 m^2/K and the proposed configuration gives an effective Aeff/Tsys of $\sim 10^4$ m^2/K at each resolution.

As the antenna station consists of a single filled aperture antenna, there is no trade-off needed between sky coverage and minimum observable elevation, except in the central compact core where the trade-off is between surface brightness sensitivity and minimum elevation. In addition, a filled aperture antenna station maximises the beam area, which in turn minimises correlator and signal transport cost.

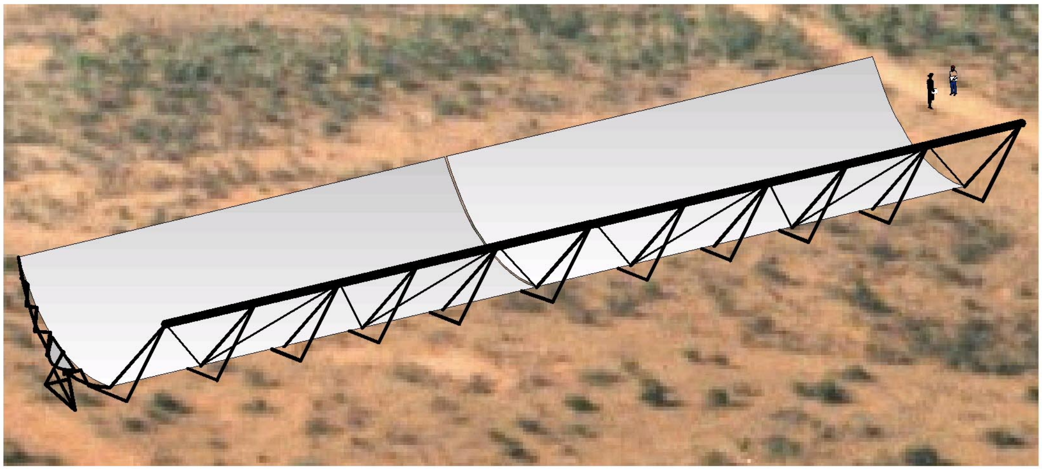

Figure 1 Cylindrical reflector antenna

A distinguishing feature of the cylindrical reflector are the multiple dual-polarisation line feeds which illuminate the cylindrical reflector. Their cost, in part, offsets savings that are made in the price of the reflector. The line feeds have a 2:1 to 3:1 frequency coverage and a number are needed to cover the full frequency range. Up to three will be active at any one time. The beamforming, Figure 2, for the linefeed is done across ~12m sections of the line feed giving approximately circular one-degree beams at 1.4 GHz.

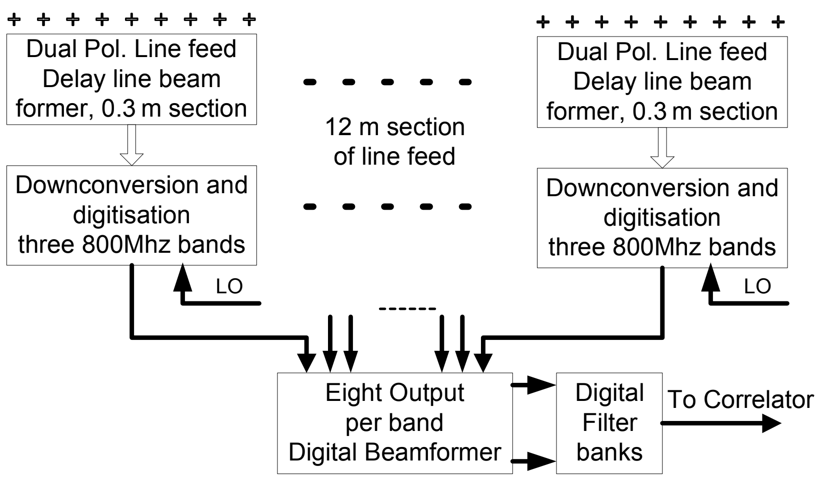

Figure 2 Line feed for a single antenna section showing analogue and digital beamforming.

The outputs from the feed elements of the line feed are amplified with uncooled LNAs and RF beamformed over 0.3m sections using a delay line beamformer. This RF beamforming reduces the arc scanned by the line feed 40^{o} at 1.4 GHz. Over a 12m section of line feed 40 RF signals are generated which are then downconverted and digitised. These 40 signals are then digitally beamformed to generate up to eight beams in each of three 800 MHz bands. The various levels of beamforming are illustrated below, at 1.4GHz the final beam size is one square degree.

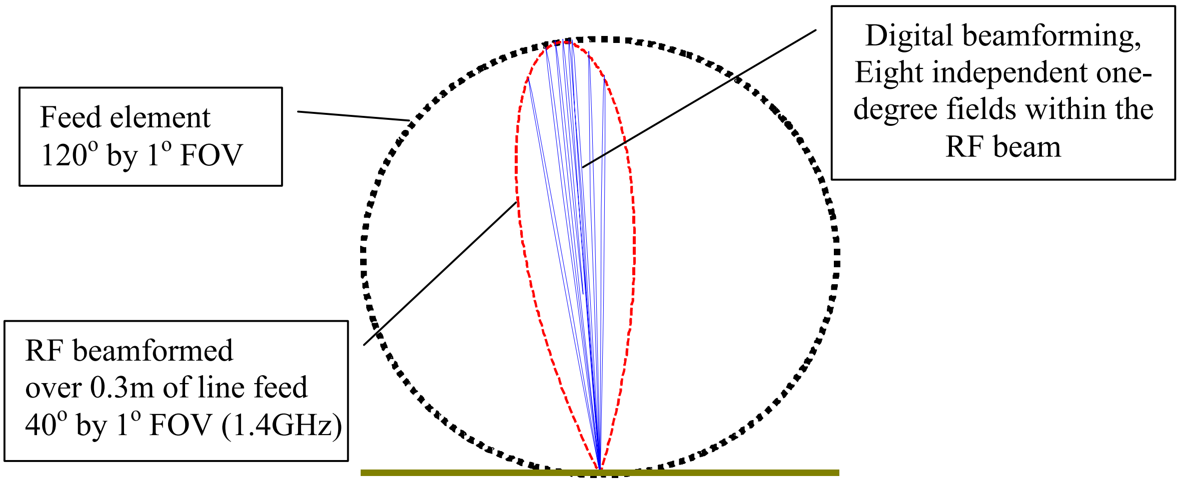

Figure 3 Beamforming hierarchy for one 12 m antenna section

The beamforming done by the reflector and RF beamformer limit the area of sky that the eight independent one-degree beams can be placed. To fully utilise the available beams automatic queue scheduling of observations is needed. This requires as few as 4,000 targets of interest at 1.4 GHz. The eight independent beams also greatly enhance the surveying capability of the instrument.

For high dynamic range imaging in a single one-degree field, the signals from the eight section of each of the 600 antennas in the SKA are correlated. The correlator is a 2.3GHz bandwidth full-Stokes correlator with 4800 inputs giving 11 million correlations. For snapshot imaging, this high correlation count gives a dirty beam with sidelobes levels of about 0.1%. Longer observations together with self calibration and the high redundancy of the array allow dynamic ranges exceeding 10^{6} to be achieved.

For other observing modes the one-degree beams from all antenna sections are beamformed and, as the reflector is contiguous, a grating lobe free fan beam can be produced. To cover the area of the eight independent beams 64 fan beams are sufficient. The correlator can form all correlations between antennas for these 64 fan beams to give a survey mode imaging capability of eight square degrees at 1.4GHz. The fan beams arrayed with other antennas are used to target compact sources.

2 Science Drivers

The wide range of science priorities identified by the SKA Science Working Groups requires that the final telescope provide both a wide frequency range and high sensitivity over a range of angular resolutions.
A concept based on cylindrical reflectors addresses the following specifications:

- Frequency coverage from 100 MHz to 9 GHz (up to 12 GHz with reduced multibeaming)
- High spatial resolution at low frequencies
- Continuous u-v coverage on scales of 10m to 3km
- Sensitivity independent of resolution (constant effective area)
- (Very) compact core configuration (specification is 0.4 km^2 within 1 km).
- Electronic beamforming giving rapid access (within milliseconds) to 120 x 1.4/*f* degrees of sky (*f*=frequency in GHz), or 8.5% of the accessible sky at 100 MHz
- Large field-of-view 56/*f* x 1.4/*f* degrees of sky
- independently over a 120-degree arc for each of line feed.
- Three independent frequency bands each steerable over 120 degrees
- Multibeaming capabilities: Can observe/image eight fields within each frequency band.

This concept matches nearly all the SKA science specifications and has exceptional advantages for studies of the Early Universe because of its high sensitivity, complete wavelength coverage and excellent spectral response in the frequency range vital to studies of cosmic HI, i.e. 100 MHz to 1.4 GHz.

We now discuss the links between the cylindrical reflector concept and the individual science drivers identified in a series of memos from the January 2002 Bologna SKA Workshop (http://www.skatelescope.org/ska_memos.shtml).

2.1 Milky Way and local galaxies

The key science drivers in this area are studies of the ISM, magnetic fields and relativistic electrons. The cylindrical reflector concept is well matched to the specifications laid down by this working group (frequency range 1 to 10 GHz, imaging field-of-view at least 1 deg^2, angular resolution 0.1 arcsec at 20cm, surface brightness sensitivity 10 mK/$arcsec^2$).

2.2 Transient phenomena

The key science drivers here are surveys of radio transients, Galactic pulsars and SETI. The cylindrical reflector concept meets all the requirements except for frequency coverage in the range 12-15 GHz which the working group states is needed to overcome interstellar scattering of pulsars near the Galactic centre.

Galactic centre pulsars will not be observable with an SKA based on the cylindrical reflector concept. However, these observations are high-risk even for an SKA which reaches to 15 or 20 GHz. The steep radio spectrum of pulsars means that their observed flux density decreases as ~ 1/frequency^2, and it is not yet clear that 15 GHz is a high enough frequency to overcome interstellar scattering near the Galactic centre. It may be necessary to go to 20 GHz or even higher, with a correspondingly large increase in the required collecting area.

The cylindrical reflector concept has the ability to image up to 8 square degrees simultaneously on shorter baselines, falling to one square deg at VLBI resolutions, making it possible to carry out all-sky surveys at arcsecond resolutions. This survey mode could provide multi-epoch radio sky maps of very large areas of sky, which would be particularly useful in studies of radio transients.

For time-critical transient events, the cylindrical reflector concept has the advantage of instantaneous access to 8.5% of the available sky at 100 MHz with electronic beam steering. With a mechanical slew rate of 20 degree/min in either direction the further part of the visible sky that can be accessed, at all frequencies, is 24% after one minute. As a result, this telescope would be able to respond very rapidly to GRB and other transient events.

2.3 Early Universe and large-scale structure

The main science driver here is observation of the Epoch of Reionisation (EoR), which requires sensitive spectral-line observations in the range 140-180 MHz. The cylindrical reflector concept meets the specifications of this working group, though we note that it may be possible to provide a substantial increase in the effective collecting area at frequencies below 200 MHz at modest cost (see section 15) if required by the science goals for EoR and high-redshift HI.

2.4 Galaxy formation

This working group has identified two key science drivers, sensitive wide-field HI surveys and deep high-resolution radio continuum surveys. These drivers have quite different configuration requirements. The former requires most of the collecting area to be on baselines less than 60 km, while the latter requires significant collecting area on VLBI baselines (~ 3000 km).

The cylindrical reflector concept can meet the specifications for the HI surveys outlined by the working group, which include both very deep surveys in redshift space and shallower wide-angle surveys. The concept is also well matched to the specifications for deep radio continuum surveys. The approximately constant 0.5-square-km geometric area at all operating frequencies sets the surface brightness sensitivity. This will allow both the detection of faint objects and high-precision measurement of their positions, which is vital for cross-identification with NGST, ALMA and next-generation optical telescopes.

Observations of redshifted CO at 10 - 20 GHz, identified as a lower-priority science driver by the Galaxy Formation working group, would not be possible with the cylindrical reflector concept. However, observations of high-redshift CO emission will be possible with the upgraded VLA (eVLA, http://www.aoc.nrao.edu/evla/) and later with ALMA.

2.5 Active Galactic Nuclei and supermassive black holes

The key science driver in this area is the cosmic evolution of the supermassive black holes, which power active galactic nuclei (AGN). The cylindrical reflector concept is well matched to the specifications needed for detecting the first epoch of AGN and starburst activity, and to studies of the radio luminosity function and its evolution.

However, detailed investigations of radio-source physics including the origin of radio jets and the properties of accretion disks requires much higher observing frequencies (up to 36 GHz) which are outside the capability of this telescope. Again, the VLBI-like requirements for this particular science goal will be realised by other telescopes such as the eVLA.

2.6 Life cycles of stars

The key science divers in this area relate to sub-AU imaging of proto-planetary disks and magnetic fields in normal stars. The specifications require high-frequency observations, with a 22 GHz capability being particularly important. The cylindrical reflector concept does not meet the specifications in this area, since its highest operating frequency is 9 to 12 GHz.

2.7 Solar system and planetary science

The cylindrical reflector concept appears to meet the specifications for solar system science, based on the discussion in the Calgary SKA Science document (Taylor, www.skatelescope.org/ska_science.shtml).

2.8 Intergalactic medium

The key science goals in this area are studies of the thermal and non-thermal components of intergalactic medium in galaxy clusters, including high-resolution imaging of the Sunyaev-Zeldovich effect and polarisation measurements. The objects to be studied include halo and relic sources, which can be extremely diffuse and exhibit structure on a wide range of angular scales from milli-arcseconds to tens of arcminutes. The proposed cylindrical reflector concept is well matched to the specifications required by this group.

2.9 Spacecraft tracking

Although it does not cover the two higher DSN bands (31-33 GHz and 37-39GHz) specified by the working group in this area, the sensitivity of the cylindrical reflector concept in the lowest band (8-9 GHz) will be 21.3 dB better than the current 70 m dishes at 8GHz. When compared to a 34 m dish operating at 32 GHz the improvement is 9.3 dB if the transmit power and size of the spacecraft antenna remains unchanged. This corresponds to a 8.5 times higher data rate, which with 8 hours of transmission per day is three times greater than that possible with the DSN 34m antennas at 32GHz. This assumes QPSK data encoding and no bandwidth limitations. If the 8GHz bandwidth was reduced by four then 16QAM could be used, limiting the data rate reduction to a factor of two. The total through put is even greater when the ability to communicate with multiple craft simultaneously is taken into account. This makes the cylindrical reflector concept an attractive option for deep space communications. In addition, the high angular resolution (equivalent to 1-2 km at the distance of Jupiter) allows precision real time tracking within the solar system.

2.10 Multibeaming

The cylindrical reflector concept described in this document provides up to eight independent beams, allowing significant multibeaming advantages. We briefly summarise the main benefits of multibeaming and argue that the SKA must have a multibeaming capability:

(1) Response: Sub-millesecond beam switching over a 120 degree arc and 24% of the visible sky available after one minute of mechanical slewing. This gives a 12% chance of rapidly acquiring time-critical events, e.g. GRBs, pulsars and the discovery of and response to new transient sources.
(2) Scheduling: A number of science priority areas which require multiple targets to be observed simultaneously (i.e. time-dependent multibeaming as opposed to simultaneous multiple users of the SKA). This science includes monitoring a pair of pulsars, timed against each other rather than using terrestrial clocks, quasar intra-day variables or quasar lensing variability.
(3) Efficiency: Having a number of independent beams (experiments) makes the SKA a true community facility with many simultaneous users and separate science projects. This will make the SKA a unique telescope, being able to spend large amounts of time on individual projects (e.g. transient sky monitoring or surveys) while other beams are dedicated to shorter, targeted observations. Multibeaming also has advantages for long-baseline VLBI-like observing modes because targets and calibrators can be observed simultaneously or, with electronic beam steering, essentially zero dead time.
(4) Sensitivity: With up to 8 simultaneous one-degree beams all being imaged simultaneously there is a eight-fold increase in integration time. This gives an eight fold speed increase when surveying or, alternatively, can be viewed as a 2.8 times increase in sensitivity. This can be interpreted as increasing Aeff/Tsys to 5.6×10^4 m^2/K.

3 Preferred Array Configuration

The SKA is a multi-resolution instrument, and with fixed-location antennas, this means that the whole of the collecting area is not available at any one baseline. A solution to generating array configurations with equal effective area at all baselines is given by Bunton [3.1]. For baselines increasing by a factor of three, it is found that the number of UV samples must increase by a fixed number for each step. For the proposed SKA array configuration with 9 baseline steps the total normalised correlation count is shown in the table below. Going from 1km to 3.15km adds 0.106 to the normalised correlation count with the 1km data providing the short baseline data. The same is true at all baselines: there is fixed fraction of 0.106 of correlations added for each baseline and the shorter baseline data fills in the centre of the UV coverage.

Table 1 Number of antennas in each baseline range.

Max Baseline (km)	1	3.15	10	31.5	100	315	1000	3150	10000
Total correlation	0.152	0.258	0.364	0.470	0.576	0.682	0.788	0.894	1.000
No of antennas	234	305	362	411	455	495	533	567	600
Added antennas	234	71	57	49	44	40	37	35	33

The number of correlations is proportional to the square of the number of antennas. To calculate the effective numbers of antennas within a given maximum baseline range multiply the total number of antennas by the square root of the normalised number of correlations. The table shows this for a 600 antenna-station design with each station consisting of a single antenna. Also shown is the number of antennas that must be added for each baseline range to achieve this.

For each increase in the maximum baseline an extra 10.6% of the total correlations is added. If only these correlations are considered then the sensitivity for each baseline would be $\sqrt{0.106} = 0.33$ of the total SKA effective area. Added to this is correlation data from shorter baselines, which can provide 40% of the UV data at any resolution; Gaussian UV coverage is assumed. This increases the effective area to $\sqrt{(0.106/.6)} = 0.42$ of the total SKA effective area. However, the short baseline data also has a 10 times higher sensitivity, further increasing the effective area to ~0.47 of the total SKA. Thus at any of the resolutions defined by the baselines from 3.15 to 10000 km, the effective sensitivity is 0.94×10^4 m^2/K

The derivation of the array configuration is given in detail in Appendix M. Here the guiding principles will be described and the results given. Within the central 1km core the large numbers of antennas allow an array with complete UV coverage and high filling factor, which in turn gives high surface brightness sensitivity. The high filling factor, however, leads to a 22-degree elevation limit, which can be reduced at the expense of surface brightness sensitivity.

For baselines greater than one kilometre most of the sensitivity is due to correlation between the distant antennas and the central core. Each of these results in zenith UV coverage in the form of the central core displace in the UV domain by a distance equal to the distance from the centre of the central core and the distant antenna. In effect, the central core is duplicated with a translation. Thus, a uniform snapshot UV coverage is achieved by placing distant antennas on a regular grid. This gives duplications of the central core on a regular grid in the UV plane. For the 1-3.15km antenna, there are sufficient antennas to allow the duplications to overlap giving close to complete UV coverage. Thus, a grading of the density of the antennas is possible, with higher densities occurring within 0.5km of the central core.

At the next maximum baseline 10km the number of antennas gives an average spacing of approximately 1.8km between antennas. This gives a UV coverage where the duplications of the central core together with the high density 3.15 km antenna abut each other, again giving excellent UV coverage. The initial design is shown below. It is seen that the initial starting array is a rectangular grid but the columns are displaced relative to each other to provide some randomisation. Also shown is the arrangement of antennas to only to one side of the central core [3.2]. This does not compromise the UV coverage and reduces cabling costs.

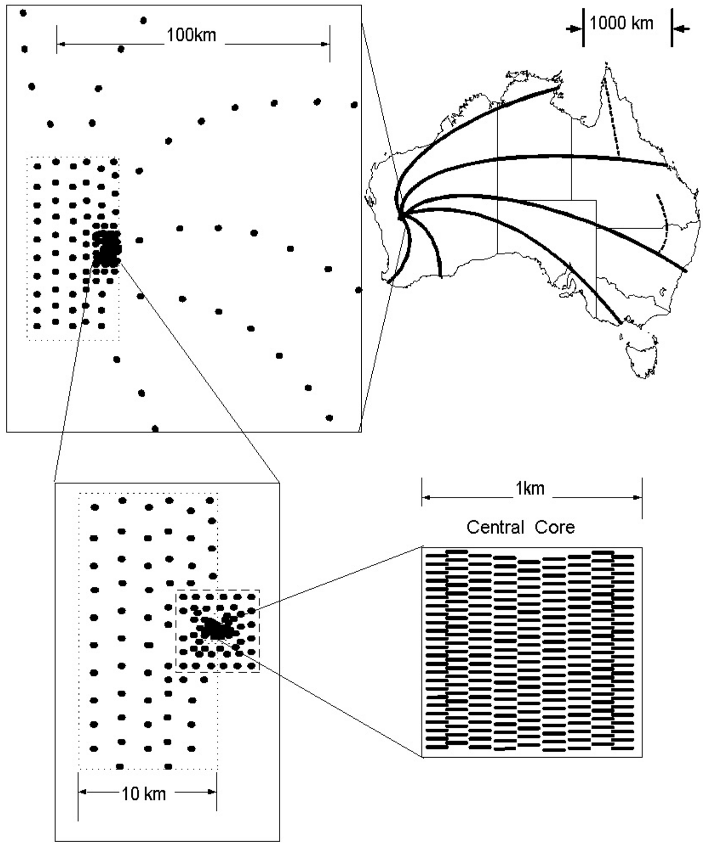

Figure 4 Possible array configuration

At the next maximum baseline, baselines to 31.5 km, there is one duplication of the central core every 38 square kilometres of zenith UV space. Complete coverage is achieved when the 3.15km antenna are added. The 31.5km-baseline antennas cover an area of 63 by 31.5km. Suitable sites for a radio quiet reserve of this size have been identified in the Australian states of Western Australia, South Australia, New South Wales and Queensland.

Beyond 31.5 km, cabling costs increase and filling the UV plane gets increasingly difficult. A set of six spiral arms could be used with eight antennas on each arm between 31.5 and 100km and seven antennas per arm from 100 to 315km. Baselines from 315km to 3150km can be accommodated within Australia with Sydney-Perth 3380km East-West and Hobart-Darwin 3300km North-South. . For purely mainland sites the maximum baselines are typically 3000km East-West and 2800km North-South. The basic layout chosen for the long-baseline antennas is a loose six-arm spiral. A possible array configuration is shown above. See Appendix J for examples of other Australian sites. Using a loosely wound spiral minimises the total cable length from the most distant antennas to the central core of antennas. In some cases existing infrastructure will be used which will lead to deviation from the current rough design. If a more closely wound spiral is used, as presented in the Luneburge Lens proposal, then greater use of existing infrastructure is needed to keep the cost of cable and trenching similar. The advantage of the more closely wound spiral is better instantaneous UV coverage. For baselines of 3000 to 6000km, antenna stations outside continental Australia would be needed. Sites such as Cocos and Christmas Island, New Zealand, Guam and Samoa are possibilities. For 5000 to 10000km baselines sites in China, India, Japan, Korea, Hawaii, Mauritius and South Africa should be considered. All these have radio astronomy communities and there are many other Pacific Islands and South-East Asian countries that might also be suitable.

4 Antenna solution

There are three main topologies possible for a cylindrical reflector: fixed reflector, vertical axis and horizontal axis. Although the horizontal axis antenna, as used at Ooty, Molonglo, Bologna and Serpukov, has been selected for this proposal, the relative benefits of the three topologies will be briefly considered.

A vertical axis design as proposed by James & Parfitt [4.1], provides the greatest astronomy benefits by allowing access to the full visible sky and minimising foreshortening. This design relies on a TiltAz mount Bunton [4.2], where azimuth coverage is obtained by use of wheel on track rotator. The reflector is tilted at about 45 degrees and full elevation coverage is obtained by electronically steering the beam. End effects, as discussed in [Appendix K], mean that the line feed must be shorter than the length of the reflector by approximately the twice the focal length. Thus, aperture efficiency becomes very low when length of the reflector is less than four times the width. As the reflector will be about 15m wide, the total length of the reflector needs to be 60 m or more.

A horizontal-axis reflector, which has been used in all existing designs [Appendix B], does not provide full visible sky coverage since it cannot scan to within 30 degrees of the ends of the antenna. However, it is still possible to have full declination coverage together with 8 to 12 hours of Hour Angle coverage. The great advantage of the design is that large apertures can be built up by joining modules edge to edge. Each module has a length approximately equal to the width of the reflector. Thus, the cost per unit area is independent of the length of the antenna as it can be built as a number of adjacent independent units.

For a vertical-axis cylindrical reflector, the cost is proportional to size raised to the power *k*, where *k* is approximately 2.7. Thus the cost per unit area of a doublet-style vertical-axis antenna is about 2.6 times that of horizontal axis design, since each doublet antenna section needs to be about 4 times larger. As a horizontal axis cylindrical reflector is expected to cost ~US$300 million, it would appear that a vertical axis design is uneconomic. The cost imposed by using a horizontal-axis design is a ~30% reduction in the visible sky that is accessible sky but no reduction in the number of sources accessible during the day. For completeness, a fuller description of vertical axis cylindrical reflectors is given in [Appendix E].

An even cheaper design uses fixed reflectors. In this design, a subreflector would be used to allow the line feed to be in focus when translated by up to 20 degrees from its centre position. In practice, the reflector would be aligned North-South and sources at elevation greater than about 30 degrees could be accessed at transit. With this design, sources at low elevations to the north and south cannot be accessed and the Hour Angle coverage is very limited. Because of the astronomy limitations this design has not been selected for this proposal. A fuller description of vertical axis cylindrical reflectors is given in [Appendix F].

The methods for constructing the horizontal axis cylindrical reflector are based on the cylindrical reflector at Molonglo [Appendix D]. Possible construction steps are listed below.

1. Build foundation and support frames
2. Install spine beam between support frames with sector gear and motor
3. Install cantilevered truss from spine beam for backing structure and line feed support
4. Attach alignment templates and line feeds
5. Install and adjust surface.

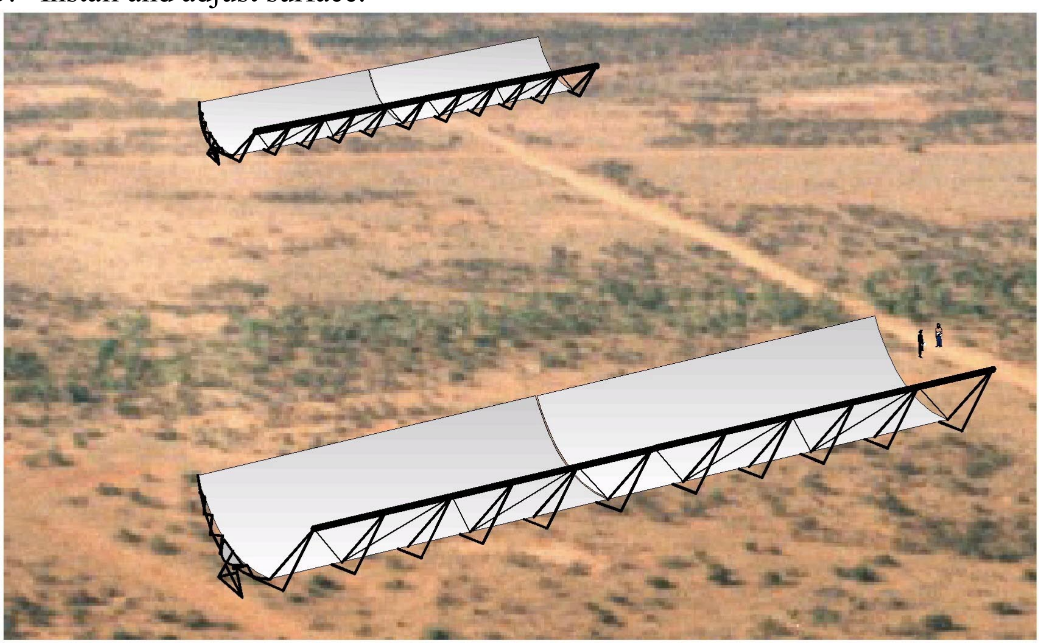

Figure 5 Two antennas of a Cylindrical Reflector SKA

4.1 Offset versus centre feed

The existing Molonglo telescope is a centre-fed reflector mounted on comparatively short support frames. The short frames simplify construction and access because all mechanical components and the reflector structure are accessible with ladders or from ground level. The limitation of such a low structure is a limited zenith angle tilt, +55 to –55 degrees in the case of Molonglo. To get zenith angle coverage down to near the horizon the support pylons need a height almost equal to half the width of the reflector. This leads to a design such as the radio-star interferometer in Cambridge and the DKR-

1000 in the USSR (picture in [4.3]) where access to the line feed and reflector is difficult. This increases the cost of construction and maintenance.

Use of an offset-fed reflector, as at Ooty and Bologna, allows an increase in the zenith angle tilt without increasing the height of the telescope. In effect, one side of the reflector has been shortened, allowing the antenna to tilt over much further on this side. Thus it is possible to build a reflector on short pylons that mechanically scans from the horizon through zenith to 60 degrees past zenith. For a reflector with the axis aligned East-West all possible declinations are accessible at transit for a telescope sited at a latitude of -30 degrees.

This allows access to 73% of the visible sky, a very attractive feature that cannot be achieved by North-South aligned designs or low height East-West centre fed reflectors. With a line feed that can scan electronically ±60º the hour angle coverage possible for a cylindrical reflector aligned East-West is at least ±4hours and ±6hours for sources south of declination –30º. The extent of this coverage is shown in Figure 6. This decreases by 1% for every 2 degrees decrease in zenith angle limit to the north. The limits of coverage are plotted in azimuth and zenith angle co-ordinates with the horizon around the edge of the circle and zenith in the centre. However, to give a better understanding of the astronomy limitations a declination DEC and Hour Angle HA grid is used.

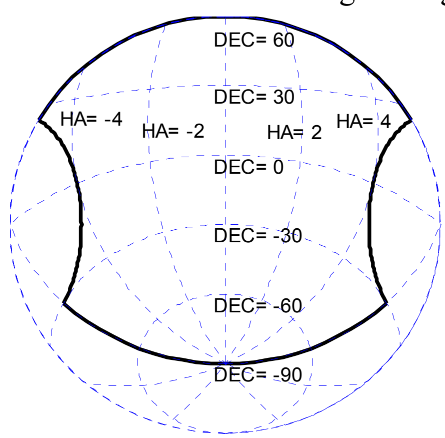

Figure 6 Possible sky coverage of East-West offset cylindrical reflector at -30º.

A short f/D offset design for the reflector as proposed by James and Parfitt 1999 [4.1] allows the feed to can be offset by three beam widths on either sided of the nominal focus. The short f/D minimises end effects and the large focal plane possible with this offset fed design allows multiple line feeds to be accommodated. An offset-fed cylindrical reflector also eliminates coupling between elements of the line feed due to reflections off the surface. Removing this coupling greatly reduces baseline ripple that can cause considerable problems in HI observations. In a centre-fed design a deliberate distortion must be made in the reflecting surface under the line feed to eliminate this problem. Finally, when the antenna is tilted over to point to the horizon, the line feed is easy to assemble because it is close to the ground. In a centre-fed design, such as Molonglo, the line feed can only be accessed by use of a vehicle-mounted cherry picker.

Thus, a low height offset-fed cylindrical reflector allows easy access to all parts of the structure, reducing construction and maintenance costs.

4.2 Antenna station design

This proposal is for a 600 antenna-station SKA, with each antenna station consisting of a single cylindrical reflector of area $1670m^2$. This makes the terms antenna and antenna station interchangeable. If a 300 antenna-station SKA is preferred, pairs of antennas can be placed end-toend and still the antenna station consist of a single filled-aperture reflector.

The cylindrical reflectors making up the station can be no more than 15m wide to achieve a one-square-degree field-of-view at 1.4GHz. As the width of the reflector is decreased the length and cost of the line feed increases. The line feed, signal processing and signal transport becomes the major cost as the upper frequency is increased. Thus, within SKA design goals, a 15m width minimises cost. With the reflector 15m wide, its lowest frequency of operation is 100MHz

The antenna, when coherently beamformed, has a highly elliptical fan beam with an aspect ratio of about 8:1. This fan beam can be designed to have low sidelobes and possibly no grating responses. The elimination of grating responses maximises the area of the fan beam. A further advantage of having a single-reflector antenna station is that there is no shadowing of one antenna by another at low elevations within an antenna station.

To form a one-square-degree image, the full length of the line feed is be broken up into eight sections. The section of reflector illuminated is approximately square and the beam formed is one square degree across at 1.4GHz. Correlating the outputs from these 4800 antenna sections gives a high dynamic range one-square-degree image. Alternatively, eight contiguous fan beams could be generated at each antenna station with each fan beam correlated with the corresponding fan beams from the other antenna stations. The one-degree image is generated as a mosaic of the 8 fan beam images. This last approach reduces the total correlator cost by a factor of eight. This reduces the total amount of information, which in turn reduces the dynamic range of the image. With a full 4,800-baseline correlator the system can be configured to image 8, 4, 2 or 1 square degree. The trade-off between these options is survey speed against dynamic range. No time sharing is needed to image the multiple fields. Thus, the effective integration time per square degree is increased by up to a factor of 8, which is equivalent to an increase in Aeff/Tsys of 2.8.

5 RF systems

The line feed is the greatest challenge in the design of a complete cylindrical antenna station, no less so than for a planar array. Using the offset fed design proposed by James and Parfitt [4.1] it is possible to place a number of line feeds, operating at different frequencies, side by side at the focus. If a line feed with a 3:1 frequency coverage can be built, then four side-by-side line feeds are needed to cover the frequency range 0.1 to 8GHz. For a 2:1 frequency coverage six or seven line feeds are need to cover a similar frequency range. This may be too large a number to fit in the focal plane in which case a rotating feed box might be used. An example of this is the feed system for the GMRT. If line feed costs are proportional to frequency and they have a 2:1 frequency coverage, then the cost of all six to seven line feeds is double that of the highest frequency line feed. For a 3:1 line feed frequency coverage the cost of all line feeds is 1.5 times that of the highest frequency line feed.

In all cases, the viability of line feeds also depends on the further development of low-noise uncooled LNAs. Research devices already demonstrate the required performance [Appendix B]. Currently uncooled amplifiers with 3:1 bandwidths at 1GHz can be built with noise temperatures of 50-60K at very low cost (a couple of US$). State of the art low-noise uncooled LNAs are reaching 20-30K and experimental devices [5.1] 14K at 2GHz. With other sources of system noise limited to 21K the experimental device allows systems temperatures of 35K to be achieve when each feed element has its own uncooled LNA.

For best sky coverage, beamforming should be fully digital, but the cost of individual downconveters and multi-bit A/D converters may not allow this. Thus, some degree of analogue beamforming is needed. As the telescope must be wideband a true-delay analogue beamformer is needed, and this will probably operate directly on the RF signal to minimise downconversion costs. At the time the SKA is constructed the RF beamforming is expected to limit the instantaneous field-of-view at 1.4GHz to about 40-60 square degrees, which corresponds to RF beamforming over a 0.3m length of line feed. With this limitation, each input to the digital beamformer corresponds to an antenna with effective area of 4.5m^2 (0.3x15m). This makes the digital beamformer about eight times the complexity of that needed for an SKA made from 6m dishes or lenses.

6 Signal encoding/transport and beamforming

At the antenna the RF beamformed signal is down converted and digitised Figure 3. A section of line feed about 0.3m in length is digitised and this data from a ~12m of line feed is digitally beamformed to form approximately circular beams. Multibit digitisers and digital processing are used to minimise losses. To save signal transport cost digitising and beamforming will be done at the antenna. If eight simultaneous beams are generated there is a five times reduction in total data rate between the input and output of the beamformer. The data is then processed by a filterbank before being encoded and modulated onto optical fibre for transport to the correlator. For interference-free channels the data is coarsely quantised as 4+4-bit complex data reducing the total data to be transmitted by a further factor of two or more. This is possible because the filterbank operations are performed at the antenna, allowing the data to be quantised to the precision needed by the correlator before transport over the fibre. With 4-bit data precision the loss in the correlator is about 1%. Channels with interference may be either deleted or encoded to a greater precision. For a 9 GHz maximum frequency the total bandwidth of each beam is 2.3GHz. Thus, the total data rate for an eight-beam system is:

2.3GHz * 8bits * 8beams * 2 polarisations* 8 12m sections = 1.74Tbits/s per antenna.

This data will be transported on ~100 light carriers with possibly individual fibres for short distances and individual wavelengths within a wavelength division multiplexed (WDM) system over long distances. To ease the correlator routing problem each light carrier will transport the data for all beams formed by the antenna over a bandwidth of approximately 20MHz. The correlator is then built as ~100 units each processing about 20MHz of bandwidth. Hardwired fibre connections together with wavelength-switching networks and will interconnect the incoming signals to the appropriate correlator unit.

7 Signal processing

Individual 12m sections will be correlated to provide data for amplitude and phase calibration of the antenna. Correlation with signals from interference mitigation reference antennas will also be made to identify interferers and help the system to steer nulls onto these interferers. This can be done at low cost at remote antenna stations. At the central site the main correlator is used. Unlike a phased array there is only one degree of freedom available for null steering. Even so, at 1.4 GHz nulling is effective over about 99% of the sky for a one-degree beam. This rises to 99.9% if the full line feed is beamformed. In addition to null steering, a small number of individual frequency channel outputs from the filterbank can be processed with adaptive noise cancellers.

The correlator is an FX correlator with the filterbank operations being performed at the antenna. Data will normally be received as 8192 frequency channels over the full bandwidth. For spectral line work, a subset of the 8192 channels can be further filtered to give high spectral resolution. This does not increase the total data rate and allows simultaneous continuum and spectral line observations. Interconnections within the correlator are minimised by use of the antenna reordering approach Urry [7.1] and the cross-multiply accumulate (XMAC) part of the correlator will use the channel reordering method, Bunton [7.2]. Channel reordering removes memory constraints from the XMAC allowing full correlations between the 600 * 8 = 4800 antenna sections. This provides a one-square-degree image based on 11.5 million baselines. About 20% of these correlations provide independent data at each resolution. This should be sufficient for snapshot images with about 10^7 pixels. If each one degree beam is known to a 1% precision then the dynamic range should be about $100 * \sqrt{(0.2 * 11.5\times10^6)} \sim 10^5$ before self calibration. With self calibration, multi-frequency synthesis and longer integrations a dynamic range of greater than 10^6 on images with 10^8 pixels should be achievable.

The beamformer will adjust the delay and phases so that the one-degree beams for the separate sections of one antenna are correctly phased for beam centre. As the outputs from the filterbanks are narrow band, the signals can form a fan beam within the one-degree beam by adjusting the phase between the different sections and adding. With eight independent one-degree fields up to 64 simultaneous beams can be generated. This number scales directly with the number of one-degree patches. For a single fan beam there are eight times fewer inputs to the correlator, reducing the correlator load by 64. Thus, the correlator can operate on all 64 fan beams simultaneously increasing the area imaged to eight square degrees. If the dynamic range is proportional to the square root of the number of correlations, the dynamic range will be reduced by a factor of eight. If this is unacceptable, the beams could be formed using four and two adjacent sections of line feed. The area imaged is four and two square degrees respectively, and the dynamic range reduced by four and two.

8 Data Management

The data rate for a given field-of-view is minimised by using a filled-aperture antenna. This occurs because with a filled-aperture antenna the beam area is maximised and this minimises the number of antenna-station beams needed to cover a given field-of-view. Fuller details are given in [Appendix C]. For a one-square-degree field-of-view, the line feed of a 111 by 15m antenna is divided into eight sections. The total data rate for one beam from the eight sections for a 2.3 GHz bandwidth is
2.3GHz by two polarisations by 4+4bits by eight line-feed sections = 294Gbits/sec.
For eight independent beams this increases to 2.3Tbits/s. Current off-the-shelf low-cost solutions for fibre optic data transmission are limited to about 1Gbits/sec. With the speed doubling approximately every year, off-the-shelf solutions should provide data rates of about 250Gbits/s in 2010 with high performance systems reaching hundreds of Terabits/s. As the SKA is a multi-resolution instrument, only the central antenna stations, which are used at all resolutions, will need a data rate of 2.3Tbits/s. For example, the antennas added to generate baselines of 31.5-100km antennas might generate only four one-square-degree beams. On VLBI baselines only a single one-degree field and a fan beam might be needed, reducing the long distance data rate to ~300Gbits/s. On intercontinental baselines the data rate might have to be reduced even further. The reduced data rates on continental baselines will significantly reduce the cost of transporting data over long signal paths. As the SKA will normally be observing many programmed sources at a number of different resolution the limitation of a single VLBI sources should impact the full utilisation of the instrument.

The more pressing problem is the data rate at the output of the correlator: 46 million correlations per integration period. Even though the filled aperture antenna minimises this number, it will still be a challenge to store and process the correlation data. If dynamic range and survey mode speed is sacrificed, the data rate can be reduced by a factor of eight.

9 Array Control, Diagnostics and Monitoring

Each antenna has only one to eight motors, making control of the mechanical components particularly easy compared to a small dish or lens option. Monitoring of mechanical integrity can be achieved with a small number of video cameras (low update rate). All other control is electronic with the major task being the suitable diagnostics to determine the performance of the line feed and RF beamformer. This will require noise sources on the dish surface with a spacing between noise sources of perhaps one fifth the focal length. This will allow the monitoring, diagnostics and calibration of the line feed for ten degree increments in meridian distance.

10 Pivotal technologies

The critical technology developments need for an SKA based on cylindrical reflectors is a high performance line feed with low-cost low-noise uncooled LNAs. The LNAs require technology developments, probably in SiGe HBT transistors, that are largely out of the control of the SKA community. Within the SKAMP project, work has started on a design of the feed elements for a line feed. This work aims to provide a line feed with good polarisation purity, stable beam shape, low baseband ripple with a bandwidth of at least 2:1. In addition, calibration techniques need to be developed and effects of inter line feed noise coupling overcome.

A technology that may significantly increase the practicality of cylindrical reflectors is radio-on-a-chip. Already the capabilities of this technology are able to meet the requirements of downconversion and digitisation of a 12 GHz signal at a bandwidth of 500 MHz (1GHz with quadrature demodulation). By building multiple systems on a single chip costs can be reduced while at the same time increasing the field-of-view.

11 Proposed SKA location

Currently ten sites in the four largest states within Australia are under consideration. The Luneburg lens proposal give further details on one of the Western Australian sites. All sited are in areas of low population density, promising a benign RFI environment. There should be minimal radiation from geosynchronous satellites as the overall population density of Australia is low. Power for the central site will probably be obtained from the local power grid. However, most of the remote sites will have to use solar power. As the design incorporates a significant fibre-optic system, there will be many opportunities for interconnection to the main communications carriers.

Other than UV coverage and RFI considerations, the main consideration in choosing between the many sites is access to a suitable nearby town to provide support for the staff of the central site.

12 Representative system performance and cost estimates

It is estimated that a cylindrical reflector will achieve an aperture efficiency of 69%. This together with a Tsys of 30K (which should be possible in 2010 with uncooled LNAs) gives an Aeff/Tsys of 2.3×10^4 m^2/K if the collecting area is 1,000,000m^2. The aperture efficiency and Tsys estimates have a high degree of uncertainty so allowing a 15% margin guarantees that the design goal of Aeff/Tsys equal to 2.3×10^4 m^2/K will be achieved. The system temperature specification is currently achievable at 1.4GHz, and by 2010 this should be achievable at 6GHz. The Aeff/Tsys will start to degrade above this frequency.

The minimum frequency is set by the width of the reflector and is about 100MHz for a 15m-reflector width. In survey mode the instrument can image up to eight square degree simultaneously. This can be interpreted as increasing integration times by a factor eight leading to the instrument having an effective Aeff/Tsys of 5.6×10^4 m^2/K. Only about 47% of this is available at any one resolution.

The area of sky instantaneously accessible is 40 to 60 square degrees at 1.4GHz, with amount available determined by the initial RF beamforming. With electronic beam steering or switching, the area accessible increases to 120 square degrees. The multiple line feeds making up the focal plane assembly are each independently steerable over 120 degrees allowing differing fields-of-view between different frequency bands. With a maximum instantaneous beam separation of 40 degrees at 1.4GHz, a 1670m^2 antenna station can form about 300 separate beams. Of these 64 are implemented in the system presented in this proposal. At all frequencies the antenna can be configured as eight separate units each generating one-degree beams at 1.4GHz. The correlator can process the 4800 one-degree beams needed to form a one-degree image. Alternatively, groups of adjacent units can be combined to generate fan beams. If N units are beamformed together then the total area that can be imaged is increased by N times.

With 4800 separate correlated elements, the dynamic range of the dirty beams can be as high as 4800:1. As this is a multi-resolution instrument, the dirty beam dynamic range is about 2000:1 for snapshot imaging. If amplitudes are known to 1% and phases to 1° then snap shot imaging dynamic range should be 200,000:1. With full synthesis, the dynamic range should exceed 1,000,000:1.

With both mechanical steering of the reflector and electronic steering of the line feed about 4-5 steradians of visible sky is accessible. Thus, the parameters of an SKA based on horizontal axis cylindrical reflectors are:

Aeff/Tsys:	**2x10^4 m^2/K**
	Up to 5.6x10^4 m^2/K with multibeaming
Frequency range:	**0.1 GHz to 9-12 GHz**
Sky coverage:	**4-5 steradians**
Imaging Field-of-view:	**1 sq deg high dynamic range mode**
@1.4 GHz	**8 sq deg survey mode (9 GHz max)**
Dynamic Range	**2x10^5 snapshot**
	Greater than 10^6 for full synthesis
Multibeam capability:	**up to 300 possible, 64 implemented (9 GHz)**
Instantaneous sky coverage:	**40 sq deg @ 1.4 GHz**
Maximum beam separation:	**40 deg @ 1.4 GHz**
	120 deg in different frequency bands

Missing from this list is polarisation purity after calibration. This is currently unknown but it is anticipated that the demonstrator at Molonglo, SKAMP, will address these issues. Other than this, the main area where a cylindrical reflector cannot meet or exceed the full SKA specification is the upper frequency limit. To reach the desired 20GHz upper frequency limit it is estimated that a cylindrical reflector SKA will cost US$1.8 billion.

12.1 Cost

The cost of a cylindrical reflector SKA is estimated in [Appendix I]. The assumptions made in calculating these cost were that Moore's law would hold for digital based technology used in the correlator, filterbanks, beamformers and radio-on-a-chip downconverters. For A/Ds and LNAs it was assumed cost would not change but that performance would double. For fibre optics the cost of short-range devices is assumed to halve every two years, long range devices every four years and optical amplifiers every eight years.

Using these approximations and estimates of current costs gives the results shown below for a 9GHz system with a reflector configured for operations up to 12GHz. Installing a surface with a higher than required accuracy allows future upgrades to 12 GHz, and with reduced aperture efficiency to 24GHz. With a reflector width of 15m the cost is about US$1 billion. Increasing the width gives a lower cost but at the expense of a reducing the field-of-view of a 12m antenna section to less than one square degree.

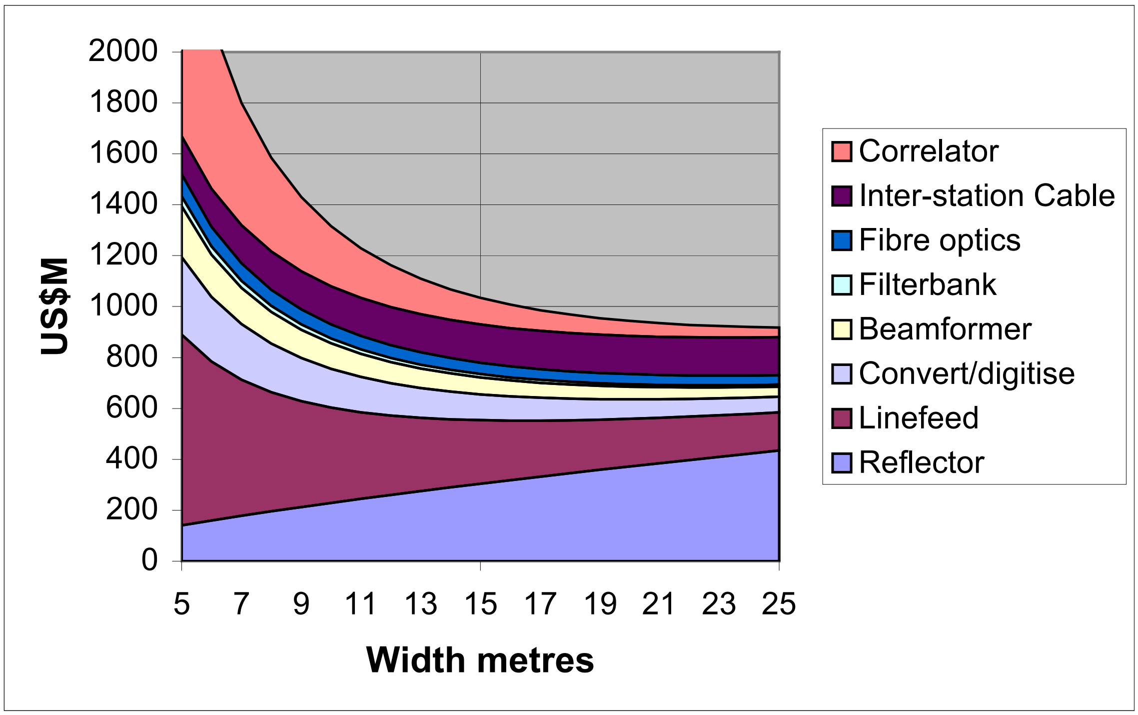

Figure 7 Cost estimates for a 9GHz cylindrical reflector SKA with a reflector designed for operation to 12GHz

For other configurations, cost can be estimated by adding the fixed cost of the reflector, line feed and cable costs given below to the costs that depend on the bandwidth processed.

Table 2 Fixed cost of reflector, line feed and cabling between stations as a function of the maximum frequency observed (millions of US$)

Frequency GHz	6	9	12	15	18	21	24
Reflector, Line feed and Fibre-Optic cable	558	676	787	894	997	1099	1199

The bandwidth cost has two components

1. Those that depend only on the bandwidth processed: downconversion, digitiser and correlator cost. This cost is US$90M per GHz of processed bandwidth.
2. Those that depend on the bandwidth processed and the average number of independent one-degree beams generated. This cost is US$9.6M per GHz per beam.

Thus if the processed bandwidth is *BW* in GHz and the average number of one-degree beams is *b* then the cost of a telescope operating to a given frequency is given by:

Cost of SKA = Fixed cost from table + 90 ****BW* **+ 9.6****BW**b*** **US$M**

For a one billion dollar cost, a 9GHz SKA could have a bandwidth of 2.2GHz with an average of six beams per antenna.

13 SKA Molonglo Prototype (SKAMP) Concept demonstrator

Funding has been obtained to upgrade the cylindrical reflector at Molonglo with technologies that show a path for possible SKA cylindrical technologies. In addition to this, the upgrade will provide significant science benefits [13.1]. In the first stage it is planned to upgrade to a full correlator and demonstrate techniques for high channel number correlators. In the second stage of the project, medium bandwidth filterbank and optical fibre interconnects will be demonstrated. In the final stage, a wideband line feed and beamformer will be installed. Development of the line feed will proceed in parallel with stage one and two developments. Current Tsys is about 75K including about 16K mesh transmission and 20K feed and beamformer loss [13.2]. Using high performance LNAs on each feed and remeshing the surface should allow a Tsys of close to 40K to be achieved with the LNA and feed element having an RF bandwidth of 0.3 to 1.4GHz (probably in two bands). Achieving the required performance in the feed and LNA will require significant effort in designing the feed and keeping the cost of the LNAs down. After the LNA, it is planned to use a 9-input RF beamformer that reduces the total number of signals to be digitised down to about 1400. The digital beamformer will produce two types of outputs. When the signal from the whole array is summed, fan beams are produced. These can be used for targeting compact sources within the 12 x 1.5 degree field-of-view (at 1.4GHz) of the RF beamformer signal. Imaging beams for an 88 input correlator are also produced. This will make the system a good demonstrator of multibeaming for SKA as well as showing the development path to a 3, 6 and possibly 12GHz wideband line feed.

By 2005 it is expected that SKAMP will demonstrate line feed and beamforming technologies suitable for a cylindrical reflector SKA as well as filterbank, correlator and signal transport technologies. When completed it will have the highest sensitivity over a 1km baseline of any instrument able to observe the southern sky.

14 Synergies with other SKA concepts

The ATA and SKAMP correlator have a great deal of similarity and collaborative links have already been established.

15 Upgrade paths for the SKA

The cylindrical reflector provides many paths for upgrading: increased maximum frequency, increased instantaneous field-of-view, increased number of one-degree beams and reduced system temperature. As mentioned above, the surface can be built to higher than the required precision and higher frequency operation added when the price and performance of uncooled LNAs becomes acceptable. An extra line feed added alongside existing ones allows simultaneous operation of the new and old systems. The same improvement in LNA performance can be used to lower the system noise in existing bands, and if operated in parallel with the existing line feeds, the field-of-view is doubled. The field-of-view can also be increased by reducing the degree of RF beamforming, which becomes viable as the cost of Radio-on-a-chip ICs, A/D converters and FPGAs decrease. The rapidly decreasing cost of FPGAs and fibre-optic components makes the addition of extra one-degree beams one of the lowest cost upgrades paths as time progresses.

A cylindrical reflector will generate significant Early Universe results at low resolutions. If more sensitivity is needed then an extra 0.5km^2 of collecting area could be added for about US$100M if the upper frequency is limited to 1.4GHz and about US$50M if the upper limit is 200MHz. Note, other technologies might be cheaper if the upper frequency is limited to 200MHz.

A strong case can be made for a full 1km^2 at VLBI baseline [15.1]. Good performance is needed on VLBI baselines to match the resolution of ALMA and new optical telescopes. This can be achieved at baselines to 3150km by quadrupling the number of 1000-3150 km antennas to 140. Although this adds only 17% to the total area, the augmentation doubles the 3150km-baseline sensitivity. Adding the extra area to existing sites allows antenna station beams to become roughly circular eight-arcminute beams and does not increase cable or site costs. The cost of the added area is about US$100M.

16 Acknowledgments

The authors wish to thank Graeme James, John Kot, Andrew Parfitt and Stuart Hay for there help with the reflector technologies, Ron Beresford for his assistance with the fibre optics systems and their costs, Russel Gough for advice on low-noise amplifiers, John O'Sullivan and Andrew Adams for information and advice on Radio-on-a-Chip technologies, Peter Hall for discussions on SKA philosophy and the SKAMP team including (Anne Green, Mike Kesteven, Duncan Campbell-Wilson, George 'Nyima' Warr, Kim Roberts and Daniel Mitchell) for their support and their efforts in progressing cylindrical reflector concepts.

In particular the authors would like to thank the reviewers Wim Brouw, Jim Caswell and Peter Hall from the ATNF, Lawrence Cram from the Australian Research Council, Graeme James from CSIRO Telecommunications and Industrial Physics and John O'Sullivan from Cisco Systems whose input has greatly enhanced this document in many areas.

17 Update History

This is an evolving document and will need updating to improve readability and add new material as it becomes available. Updates listing major changes are given below

11 July 2002

Review by Peter Hall found the document hard to follow and recommended the addition of material to clarify a number of points. This involved the deletion of some unnecessary detail, the correction of many typographic errors and the addition of explanatory text. In some cases there were major changes:

- Section 1.1 material on progress needed in line feed technology.
- Section 1.2 rewritten for greater clarity with the addition of two figures.
- Section 3 addition of figure showing array configuration at 4 different scales and the removal of some detailed material to Appendix M.
- Section 4 greater emphasis on horizontal design in introduction.
- Section 7, Appendix K and Appendix H. Rough analysis of aperture efficiency and spillover undertaken. Analysis in agreement with published data and aperture efficiency was revised down to 69%. This was compensated by the analysis giving an estimate of spillover. New spillover used to give better estimate of Tsys leading to an overall improvement in Aeff/Tsys.
- Appendix I. Better derivation of cost estimates requested - lead to updated estimates and slight increases in total costs.
- Appendix L Compliance table based on the US model added.

In addition to this,

- A better understanding of the beam sizes of arrays was discovered which has resulted in Appendix C being updated.
- Reviewer list to acknowledgments to better conform with presentation of other documents.

18 References

[1.1] Bregman, J.D. 'Concept design for a low frequency array', in H.R. Butcher (ed) , SPIE Astronomical Telescopes and Instrumentation 2000 - Radio Telescopes, Vol. 4015, SPIE, Bellingham, March 2000.

[3.1] Bunton, J.D., '"Fair" UV Coverage for a Multi-resolution Telescope', SKA workshop, Technology Pathways to the Square Kilometre Array, 3rd-5th August 2000, Jodrell Bank Observatory, UK, http://www.jb.man.ac.uk/ska/workshop/

[3.2] Bunton, J.D., 'Array configurations that tile the plane' Experimental Astrophysics Vol 11, No3 pp193-206, 2001

[4.1] James, G.M. & Parfitt, A.J., 'A Low-Cost Cylindrical Reflector for the Square Kilometre Array', in Perspectives on Radio Astronomy: Technologies for Large Antenna Arrays, (eds.) Smolders &. van Haarlem, ASTRON, 1999
[4.2] Bunton, J.D. 'TiltAz Mounted Antenna', The SKA: Defining the Future, Berkeley Workshop, July 2001 http://www.skatelescope.org/skaberkeley/
[4.3] Steinberg, J.L., & Lequeux, J. 'Radio Astronomy' translated by Bracewell, R.N., McGraw-Hill 1963
[5.1] Niu, G. & Zhang, S. 'Noise Modeling and SiGe Profile Design Tradeoffs for RF Applications', IEEE Trans on Electron Devices, **47**(11), p 2037, Nov 2000
[7.1] Urry, L.W., 'A Corner Turner Architecture', ATA Memo 14, November 2000, http://astron.berkeley.edu/ral/ATAMemo14.pdf
[7.2] Bunton, J.D., 'Low Cost Cross Multiply Accumulate Unit for FX Correlators' ALMA Memo 392, Nov 2001,
[13.1] Green, A.J., Bunton, J.D., Campbell-Wilson, D., Cram, L.E., Davison, R.G., Hunstead, R.W., Mitchell, D.A., Parfitt, A.J., Sadler, E.M., Warr, G.B. 'Prototype SKA Technologies at Molonglo: 1. Overview and Science Goals', The SKA: Defining the Future, Berkeley Workshop, July 2001 http://www.skatelescope.org/skaberkeley/
[13.2] Private communication Duncan Campbell-Wilson
[15.1] Porcas R. & Garrett, M., 'High Resolution SKA Workshop Report', Bologna SKA Workshop "New Frontiers in Astrophysics" (Jan 14-182002) http://www.euska.org/workshops/hr_ws_MPIfR_Bonn.html

Appendix A

Costing of Existing Telescopes

John Bunton
CSIRO Telecommunications and Industrial Physics

Costs are available for a number of radiotelescopes including the cylindrical reflectors at Molonglo. These are shown in Table 3. These figures allow a comparison of the relative cost of various alternatives to be found by calculating the cost of the telescope in current dollars then adjusting this to find the effective cost of a 100m^2 antenna. This then gives a relative measure to estimate the cost of a cylindrical reflector.

Table 3 Costs of a number of radiotelescopes in current dollars.

	Year Complete	Cost US$k at completion	conversion to US$	Inflation to 2002	cost US$M 2002	Cost per 100m^2 US$k
ATA[13] note 1	2001	US$30	1	1.03	31	109
Lovell [1]	1957	£st630	2.8	10	17,640	389
Parkes [2]	1961	US$1100	1	9.3	10,230	318
Effelsberg [3]	1972	DM34000	0.31	7.3	76,942	980
GBT [4]	2002	US$100000	1	1	100,000	1155
VLA [5] note 2	1980	US$78600	1	7.3	573,780	4329
VLBA [13] note 1	2001	US$3000	1	1.03	3,090	629
Radioheliograph [5]	1967	US$630	1	8.3	5,229	37
Molonglo [7,18] note 3	1967	US$600	1	8.3	4,980	13
GMRT (Dish) [8]	1996	US$400	1	1.35	540	34

note 1 Estimated cost for a single reflector.
note 2 in 1972 dollars although some references give it as 1977 dollars [9] this would reduce the 2002 cost by 18% to about US$470M
note3 The price given in [7] is US$746k, this included cost other than the construction costs. Actual construction cost was closer to US$600k as remembered by Bernie Mills [18]

Table 3 gives cost at time of completion. This cost is converted to US$, using the exchange rate at the time of completion and is then adjusted for United State inflation to bring the cost current dollars. Inflation was calculated using the values obtained from [10] and it has been used as an indicator for price increases because a significant part of the cost is labour, and labour costs rise faster than the normal indicator of price change, the consumer price index (CPI).

Table 4 Inflation for the United States

Years	Inflation % per year	Change over period	Cumulative change to 2002
1957-59 (est)	1.92	1.06	10.0
1960-69	1.92	1.21	9.50
1970-79	3.36	1.39	7.85
1980-89	11.68	3.02	5.64
1990-99	5.50	1.71	1.87
2000-02	3.00	1.09	1.09

The costs shown in Table 3 are for telescopes of different sizes and number of antennas. To allow a fair comparison the cost of a 100m^2 reflector is calculated. First, the cost of a single antenna is calculated and scaled to that of antenna of 100m^2 collecting area (diameter = 11.3m). When Parkes was being designed, it was estimated that cost was proportional to diameter raised to the power 2.5[14], this is also the figure quoted by Swarup [8]. More recently, a figure of diameter raised to the power 2.7 has been used [15] [16] and even diameter cubed [17]. For the work here a cost proportional to diameter$^{2.7}$ will be used, as this gives the best agreement between the results. For example, the ATA cost after scaling by the diameter cubed relationship and adjusting for the frequency differences is three times the cost of the GBT. For Molonglo it is assumed that nominal width is 12m. Using this an area equivalent to that of Molonglo can made up of 345 12m parabolic dishes. The results of the calculations using these assumptions are show in Table 5.

Table 5 Cost of a 100m^2 antenna based on cost for existing telescopes.

	Diam. M	No. of units	Area/unit m^2	Cost 2002 US$M	Cost/unit 2002 US$M	100m^2 2002 US$k cost $\propto d^{2.7}$	Fmax GHz Note	Scaled by cube root of Fmax
ATA	6	1	28	0.031	0.031	170	11	77
Lovell	76	1	4536	17.6	17.6	102	3	71
Parkes	64	1	3217	10.2	10.2	94	3	65
Effelsberg	100	1	7854	76.9	76.9	213	25 [11]	73
GBT	105	1	8659	100.00	100.0	242	100	52
VLA	25	27	491	573.8	21.2	2481	24	860
VLBA	25	1	491	3.09	3.09	361	24	98
Radio-heliograph	13.7	96	147	5.2	0.054	32	.16[2]	59
Molonglo	12	345	113	5.0	0.014	12	1.4 [12]	10.9
GMRT(Dish)	45	1	1590	0.540	0.540	13	1.7	10.8

Note: maximum expected frequency of operation when telescope commissioned.

[2] The radioheliograph operated at a maximum frequency of 327MHz, which was well beyond the design of the reflector. However, as the sun is such a strong source it still had sufficient effective area.

Some comparisons show that this method gives reasonable results. Both Effelsberg and the GBT have similar size and performance and it seen they have similar costs in current dollars even though they were built almost 30 years apart and funded in different currencies. The GBT is costlier but operates at a higher frequency and incorporates an active surface. Lovell and Parkes are also similar in size and performance and again the scaled costs of the $100m^2$ dish are similar. In this case, there is very little difference in the inflation but two were funded in different currencies. The differences between Lovell/Parkes and Effelsberg/GBT are due to the higher initial operating frequencies of the latter. This difference is approximately modelled by scaling the cost by the cube root of maximum frequency. When this is done most of the parabolic dishes have a scaled cost of US$50-75k for a $100m^2$ 1GHz antenna.

The most expensive design in the group is the VLA with a cost, for similar sized antennas, that is 11 times that of Effelsberg. The factors that increased the cost were mainly associated with items other than the antenna: mobility, the rail track, signal distribution and correlator. This is clearly seen when the cost is compared to that of a VLBA antenna, which is only slightly more expensive than Effelsberg. The extra investment in the VLA led to significant astronomical benefits: resolution up to 30 times greater, an imaging area 16 times greater and most importantly 350 times as much information (proportional to the size of the correlator). The increase in information is so great that snapshot imaging became possible. With the SKA the imaging area will be at least 4 times greater and the amount of information at least two orders of magnitude greater. But the cost of the VLA, about half a billion US$ in current dollars, makes it a poor model to follow for the SKA. In terms of antenna technology, only Molonglo and the GMRT provide acceptable antenna cost.

Note, the cost of SKA antenna elements, in millions of US$, is found by multiplying the numbers in the last column of Table 5 by 10. Thus using Parkes-type 11.3m dishes makes the cost of SKA antennas about US$650M for a 1GHz instrument. For Molonglo or GMRT approaches, the cost could be about US$110M. Govind Swarup estimated a cost of US$250M for a GMRT design working to 5GHz, which is close to the expect cost if it is proportional to the cube root of frequency. For a 10GHz Molonglo style cylindrical reflector the cost is estimates to be US$240M assuming the extrapolation from the original Molonglo cost is valid.

However, there are some complicating factors: half the area of the original Molonglo did not move and like the VLA, it had a significant signal distribution system and "correlator" costs and in addition, it needed 3km of line feed. The non-moving part of the Molonglo reflector is estimated be half the cost, per square meter, of the moving elements. This increases the relative cost of a moveable Molonglo-style reflector by 33%. Next, the cost must be reduced by the cost of line feeds, cabling and electronics. The ~150kms of coaxial cable is estimated to account for 10% of the cost. The North-South line feed with its ~4000 mechanical phase shifters probably cost at least this amount. Then there are the 199 downconverter and IF systems, 177 analogue 4.4µs variable delay lines and 11 beamformers and analogue correlators. When all this is considered it is seen that in actual fact the antenna cost of US$10,900 per $100m^2$ is probably an overestimate of the cost of a Molonglo-style cylindrical reflector.

[1] Robertson, P. 'Beyond Southern Skies', Cambridge University Press 1992 p140
[2] Robertson, P. 'Beyond Southern Skies', Cambridge University Press 1992. p121-125
[3] http://www.mpifr-bonn.mpg.de/public/eff_e.html
[4] initial funding $75M but estimated to cost ~$100M in current dollars
[5] http://www.aoc.nrao.edu/pr/vla20.html
[6] Robertson, P. 'Beyond Southern Skies', Cambridge University Press 1992 p190
[7] Robertson, P. 'Beyond Southern Skies', Cambridge University Press 1992. 194
[8] http://www.atnf.csiro.au/projects/ska/WS/wsswarup/
[9] Napier, P.J., Thompson, R. and Ekers, R.D., "The Very Large Array:…" Proc IEEE vol 71, No 11, p1295, Nov 1983.
[10] www.globalfindata.com/articles/Century_of_Inflation.doc
[11] Hachenberg, O., Grahl, B.H. and Wielebinski, R., "The 100-Meter Radio Telescope at Effelsberg" Proc IEEE vol 61, No 6, p1288, Sept 1973.
[12] Mills, B.Y., "The Molonglo Observatory Synthesis Telescope", Proc. SA, Vol 5, No 2, pp156-159, 1981
[13] Weinreb, S., Bagri, D., 'Progress at JPL concerning Antenna and Wideband Receiver Design', SKA: Defining the Future, Berkeley 2001, http://www.skatelescope.org/skaberkeley/
[14] Robertson, P. 'Beyond Southern Skies', Cambridge University Press 1992. p153
[15] Dreher, J. 'The Allen Telescope Array', SKA: Defining the Future, Berkeley 2001, http://www.skatelescope.org/skaberkeley
[16] Wilkinson, P.N., 'The Hydrogen Array', Radio Interferometry: Theory, Techniques and Applications IAU Colloquium 131, ASP Conference Series, Vol. 19, 1991 T.J. Cornwell and R.A. Perley (eds.) , pages 428-432.
[17] Weinreb, S., D'Addario, L., 'Cost Equation for the SKA' SKA EMT Memo 1, 2001, http://www.atnf.csiro.au/projects/ska/emt/Knowledge_Bank/Documents/documents.html
[18] private communication Bernie Mills

Appendix B

Historical Perspective

John Bunton
CSIRO Telecommunications and Industrial Physics

Around the time of the 1960s a number of large cylindrical reflector telescopes were built. These telescopes used a horizontal axis of rotation. The cost of such a reflector increases linearly with area and in one plane the reflector is flat and can be made by stretching wires between trusses. This gave an exceedingly economical design at low frequencies but only one linear polarisation can be received. To overcome this problem the wire can be replaced by horizontal supports or purlins mounted on regularly spaced trusses. This provides support for wire mesh or metal sheeting.

The four major stretched wire cylindrical reflectors built were:

- The Radio-Star Interferometer built at Cambridge, England and fully operational in 1958 Ryle [1]. This telescope operated at a frequency of 178Mhz using a 4442x20m steerable reflector together with one moveable 58 x 20m reflector. The actual cost of the reflector was two pounds per square meter Ryle [2] or about US$56 at current prices. This would make the cost of the reflector for a low frequency single polarisation SKA about US$56milion.
- The DKR-1000 built at Serpukhov, USSR. The details of this are only available from a Russian paper. Artyuk et al. [3] describe it as a parabolic cylinder with a 1000 x 40-m rectangular aperture in the form of an east-west array. It was steerable in declination and appears to be of a stretched wire design. Since then a north-south arm has been added [4]. A picture of this telescope can be found in the book by Steinberg and Lequeux [11] and [4].
- The Ooty Radio Telescope was completed in 1970 at Ootacamund, India Swarup [5]. It operates at a frequency of 327Mhz with a 530 x 30m offset-fed reflector. The antenna is orientated North-South on the side of a hill with an 11-degree incline. With this the axis of the antenna points to the poles and Hour Angle tracking of sources is achieved by mechanical rotation of the antenna.
- The Northern Cross at Bologna, Italy. Completed in 1967, this telescope operates a frequency of 408Mhz with a 600 x 35m offset-fed reflector and sixty four 24 x 7m antenna arranged in the form of a T. [6]

In addition, one major telescope using mesh supported on purlins was completed at Molonglo, Australia in 1967 Mills [7]. This telescope initially operated at 408 MHz as a transit instrument with dual mechanically steerable 778 x 12m reflectors placed on an East-West line forming a cross with a non-moving North-South cylindrical reflector, total collecting area 38,000m^2. The spacing of the purlins could permit operation up to 2 or 3GHz using a fine-weave mesh. The dual mechanically steerable antennas, with an area of 18,000m^2, were upgraded in 1980 for operation as a synthesis telescope at 843 MHz.

Many other reflector technology radiotelescopes were built in the late fifties and sixties, some of these are listed in Appendix A and a list of synthesis telescopes appears in Napier et al. [8]. Of these, the largest collecting areas belong to telescopes using cylindrical reflectors. Why then have the single and multi-dish radiotelescopes been so popular and successful even though the collecting areas can be smaller by an order of magnitude or more? It can be argued that the reason for this is the cost and performance of electronics. Firstly, there is the cost of the LNAs. In 1970, an uncooled bipolar transistor LNA might cost US$100 (current dollars) and have a noise temperature of 300K and a parametric LNA about US$10,000 with a noise temperature of 50K. Equipping single and multi-dish radiotelescopes with parametric LNAs was affordable but a cylindrical reflector radiotelescope with hundreds of LNAs could at best use an uncooled bipolar transistor. Thus, the increase in Tsys of cylindrical reflector telescopes largely negated the increase in sensitivity due to the large area. Added to this is the comparative cheapness of installing a new feed system on parabolic dish radiotelescopes. Especially on single dish radiotelescopes there has been a continual evolution in receiver design with modern cooled LNAs achieving hundreds of MHz of bandwidth and total system temperatures of ~20K at 1.4GHz (LNA noise temperature much less than 10K). These modern receiver systems may be expensive but continue to be a viable investment because of the improvement in the performance of the telescope.

In contrast, upgrades of cylindrical reflector radiotelescopes are exceedingly rare because the number of LNAs can be very large. For example, the upgrade Molonglo Large [9] required 372 new LNAs. The steerable beamforming network is an added cost in a cylindrical reflector radiotelescope. One of the first was installed on the North-South arm of the 408MHz Mills Cross. This was a complex and costly mechanical design, which needed considerable skill for correct operation. Ooty [5] also used mechanical phase shifters and the current Molonglo radiotelescope Large [9] uses mechanical rotation of the feed together with electrical phase shifting on each waveguide output. The use of phase shifting to steer the beam has limited most cylindrical reflectors to narrow band operation and the mechanical nature of the phase shifters has made a change in frequency difficult. Thus while single dish and many multi-dish radiotelescopes have seen a continual improvement in bandwidth, number of frequency bands, and system temperature, the same is not true of cylindrical reflector antennas.

B.1 SKA Perspective

Do the problems that have historically limited cylindrical reflector radiotelescopes affect the adoption of cylindrical reflectors for the SKA? The answer to this is no, especially at lower frequencies, because of advances in device technology and the requirements of the SKA. For all designs there is the requirement that the SKA has a one-square-degree field-of-view at 1.4GHz. This translates into the requirement that the antenna system have at least 4,300 independent feeds Bunton [10]. The number of feed and associated LNAs is largely independent of antenna type and it is seen that all designs for the SKA will suffer from the problem that upgrades to the feeds and LNAs will be expensive.

Historically, cylindrical reflectors have also had higher system temperature, which in the 1960s could be as much as six times higher than a telescope using cooled receivers. But it is seen in Figure 8 that the actual noise temperature of uncooled LNAs has been decreasing steadily with time. This is now improving the relative performance of radiotelescopes using uncooled LNAs because contributions to the system temperature such as spillover and sky noise are starting to dominate. In the future, there will be little difference between the performance of cylindrical reflectors using cooled LNAs and other technologies. These issues are discussed further in the section on LNAs [Appendix H].

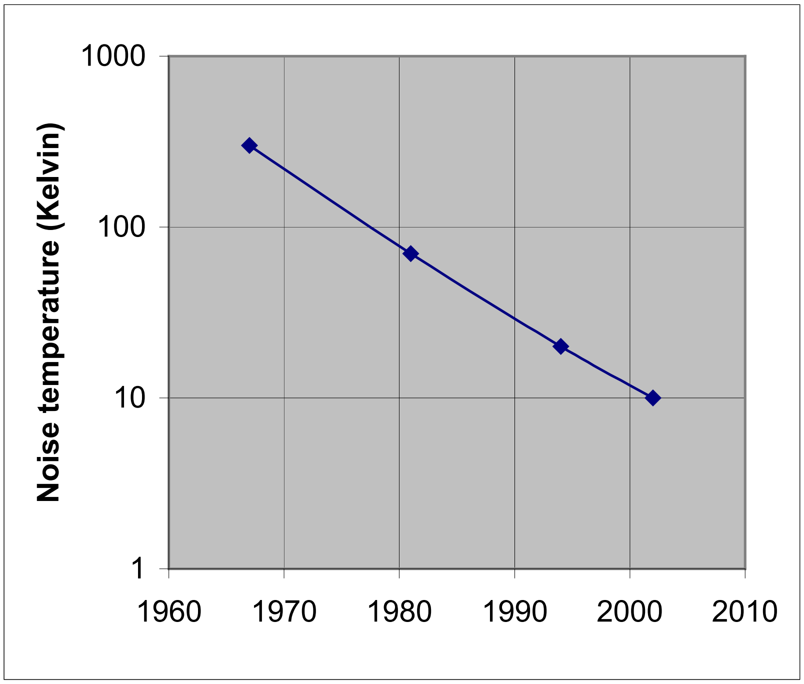

Figure 8 Improvement in uncooled LNA over time from Westerbork 1.4GHz in 1967, Fleurs 1.4GHz in 1980 to Molonglo 0.84GHz in 1994 and 2002.

The area where the cylindrical reflector excels for the SKA is minimisation of data transmission and correlator cost. As the reflector can be built as a filled aperture antenna the area of the beam generated is maximised. This minimises the number of beams needed per antenna station to provide a one-degree image. When antennas are arrayed, there is a decrease in the filling factor [Appendix C]. This reduces the area of the beam, after beamforming of the array elements. Thus, more beams are needed to cover a given area of sky leading to increased signal transmission and correlator costs compared to a filled aperture antenna of the same size.

B.2 Conclusion

In many eyes cylindrical reflectors have been considered to be a technology that has had its day with current telescopes dating from the 1960. Above it is shown that high number of feed elements and beamformer limitations and cost led to instruments that had a high Tsys, were narrow band and relatively inflexible. Even so, because of the low reflector cost they were still an attractive option. For the SKA the decreasing noise figure of uncooled LNAs will mean a reduction in the relative Tsys disadvantage from about 6:1 to less than 2:1, thereby greatly diminishing a major disadvantage of cylindrical reflectors.

Digital beamforming allows operation of wide bandwidths eliminating a second disadvantage. Finally, wideband line feeds (effectively providing continuous frequency coverage from 100MHz to 9GHz or greater) together with the rapidly decreasing cost of digital beamforming, eliminates the inflexibility of previous designs. Thus, a cylindrical reflector SKA reaps the advantage of cheap reflector technology without any of the disadvantages of previous designs and provides a wider field-of-view and greater multibeaming capabilities than are possible with any of the designs based on parabolic dish reflectors. In addition, the ability to form large filled aperture antenna minimises signal transmission and correlator costs.

References

[1] Ryle, M. 'The Mullard Radio Astronomy Observatory', Journal IEE **6**, pp14-19, 1960
[2] Ryle, M. ' Telescopes of Large Resolving Power', Science 188, p1017-1079, 1975
[3] Artyukh, V.S., Vitkevich, V.V., & Dagkesamanskii, R.D., 'Radio Spectra at Meter Wavelengths', Soviet Astronomy –AJ **11**, pp 792-799, 1968
[4] http://www.prao.psn.ru/english/3.html
[5] Swarup, G. et al. 'Large Steerable Radio Telescope at Ootacamund, India', Nature Physical Sciences **230**, pp185-188, 1971 and also http://www.ncra.tifr.res.in/ncra_hpage/ncra/ncra.html
[6] Web 1, references for Northern Star telescope from the web http://tucanae.bo.astro.it/pulsar/bolsurvey/croce.html and http://www.ira.bo.cnr.it/ira-docs/overview.html
[7] Mills, B.Y., Aitchison, R.E., Little, A.G. and McAdam, W.B., "The Sydney University Cross-type Radio Telescope", Proc. RE Aust., vol 24, p156-164, Feb. 1963
[8] Napier, P.J., Thompson, R. and Ekers, R.D., "The Very Large Array: Design and Performance of a Modern Synthesis Radio Telescope", Proc IEEE vol 71, No 11, p1295, Nov 1983.
[9] Large, M.I., Campbell-Wilson, D., Cram, L.E., Davidson, R.G. & Robertson, J.G. 'Increasing the Field Size of the Molonglo Observatory Synthesis Telescope', Publ. Astron. Proc. Australia **11**, p44, 1994
[10] Bunton, J.D., 'SKA antenna Selection, Economics and the Field of View', SKA workshop, Technology Pathways to the Square Kilometre Array, 3rd-5th August 2000, Jodrell Bank Observatory, UK, http://www.jb.man.ac.uk/ska/workshop/
[11] Steinberg, J.L., & Lequeux, J. 'Radio Astronomy' translated by Bracewell, R.N., McGraw-Hill 1963

Appendix C
Cost of an Imaging Correlator for the SKA

John Bunton
CSIRO Telecommunications and Industrial Physics

C.1 Introduction

This memo analyses the cost of FX correlators that meet the performance required by the SKA in terms of field-of-view. It is assumed that an FX correlator will be used and the cost will have two main components: the frequency transform and the cross multiply accumulates. It will be shown that the cost of the frequency transform depends only on whether the antennas are arrayed or not and the cost of the cross multiply accumulate depends on the degree of mosaicing.

C.2 Reference correlator

The specifications for the SKA require a one-square-degree imaging beam at 1.4GHz and total correlator bandwidth of 1-4 GHz with dual polarisation. There are two cases to be considered:

1. Use filled aperture antennas such as phased arrays, LAR, KAST and cylindrical reflectors that have a beam sizes less than or equal to the 1 square degree
2. Use arrays of smaller antennas.

The one-degree field-of-view antenna can be treated as the simplest case of the filled aperture antenna. A 190m^2 parabolic reflector gives a 1-degree field-of-view at 1.4GHz[3]. An SKA built from these has 5250 antennas. One way of generating the data for an image is to correlate all 5250 stations in a correlator. This can be considered as the reference cost of a correlator. It has 5250 signal that must undergo a frequency transformation and cross-multiply accumulation (XMAC) must be formed on 13 million baselines.

C.3 Filled aperture antenna stations

For filled aperture antennas with areas greater than 190m^2, the one-degree image is generated by forming a mosaic of a number of subfields. If the antenna area is increased by a factor *k* then the beam area decreases by 1/*k*. To achieve the one-square-degree imaging area each antenna must generate *k* beams. However, the increase in antenna size has reduced the number of antennas by the same factor. Thus, the total number of signals into the correlator is unchanged but is now composed of *k* signal from 5250/*k* antennas. For filled aperture antennas the data transmission and filterbank load is independent of the size of the antenna as long as its field-of-view is less than one degree. In contrast, the

[3] Derived by scaling from 1.4Ghz beam size of the 64m Parkes multibeam, 14.4 arcmin, and the 100m Effelsburg antenna, 9.4 arcmin.

cost of XMACs decreases in direct proportion to k. A separate correlator is now needed for each beam but has only $5250/k$ inputs. Thus, this correlator is smaller than the reference correlator by a factor of $1/k^2$. (Correlations between adjacent beams to correct for 2nd order effects have not been included but will be needed for high dynamic range imaging.) To form the full one-degree image there are k of these correlates so the total cost of the correlator is $1/k$ that of the reference correlator.

C.3 Antenna station arrays

For a regular array of antennas, the costs increase because the area of the beam when all the elements are arrayed together is small than that of a filled aperture antenna with the same effective area. If grating lobes are ignored then the decrease in main beam area gives a proportionate increase in the number of beams that must be processed to generate the required one-square-degree image. The increase in signal transport and correlator cost is directly proportional to the increase in the number of beams. The increase in cost depends on the minimum elevation angle observed and antenna-element aperture efficiency. The equation defining this increase in cost, derived in section C.5, is plotted below.

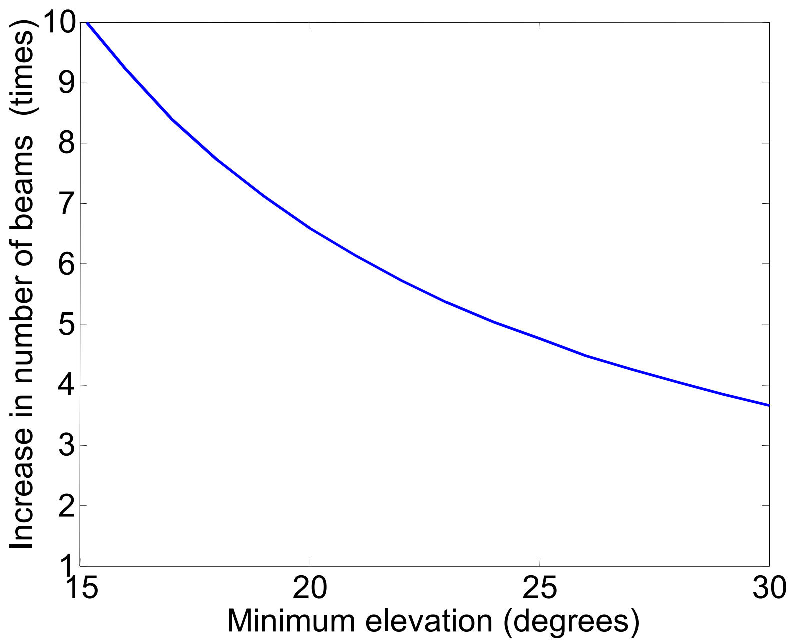

Figure 9 Increase in number of beams needed to cover one square degree when a fully beamformed array is substituted for filled aperture antenna assuming 100% aperture efficiency.

It is seen that the cost of the correlator can increase by a factor of about 10 for a minimum elevation of 15 degrees. If the effect of aperture efficiency η is included, this increases to 14 for $\eta=0.7$. For a minimum elevation of 30 degrees, the increase is about five after aperture efficiency is included. The increase in the number of beams that must be simultaneously processed means that the cost of the XMACs and filterbanks both increase by this factor.

C.4 Conclusion

Correlator costs are dependent on the number and type of SKA antenna stations. Increasing the number of antenna station increases the cost of XMACs but leaves the cost of filterbanks and signal transport unchanged. Cost also depends on whether the antenna station is operated as an array or filled aperture antenna. For a given antenna station size, using an array instead of a filled aperture antenna increases correlator and signal transport costs. The cost increase ranges from a factor of about 4 with a minimum elevation of 30 degrees, to 12 and more for elevations below 15 degrees.

C.5 Beam width and average beam area of an array

In this section the beam width of an array of hexagonally packed antenna is calculated. To satisfy minimum elevation requirements these antenna must be spaced apart leading to an increase in the size of the array and a reduction in beam width. This is a function of the minimum elevation and the number of antenna in the array. This beam width is then compared to that of a filled aperture antenna to give the ratio of the number of beams in each case needed to image the same area of sky. Finally, this ratio is average over all elevations available to give the relative cost of correlators and signal transport in the two cases.

Consider a circular array of antennas with the same total area as a single circular filled aperture antenna of radius R. For observations at zenith, the array of antennas can have their edges touching and the minimum area configuration corresponds to hexagonal packing. For the limiting case the area covered by the array is greater by a factor equal to the ratio of a hexagon to a circle inscribed within it: that is 1.1. As the minimum elevation without blockage is increased as distance between elements of the array increase in direct proportion to 1/sin(elevation). Thus the total area of the array of hexagonal areas is $\sim 1.1/\sin(\text{elevation})^2$ greater than the area of the filled aperture antenna.

The area the hexagons can be used to calculate the beam size. This has been shown for the one-dimensional case where the beam width of an array of point elements has been matched to that of filled aperture. Empirical results for unit spaced elements is shown below

Number of unit spaced elements	2	5	10	20	50	100
Width of equivalent filled aperture	1.8	4.9	10	20	50	100

Thus the effective width of the array is approximately equal to the spacing between elements times the number of elements. This is true even though the end-to-end length of the array is one less. This result can be extrapolated to two-dimensional rectangular arrays because the array can be decomposed as the convolution of two orthogonal one-dimensional arrays. With unit spaced elements in an mxn grid it is found that a uniformly illuminated filled aperture of dimensions mxn has the same beam size. From this is can be inferred that the effective radius of the circular hexagonal-grid array is:

$$\text{Radius of array} = \frac{R\sqrt{1.1}}{\sin(\theta)}$$

For a filled aperture antenna the beam width is approximately 1.09 λ/(effective diameter) where the effective diameter is the diameter of a circle of area equal to that of effective aperture. If the filled aperture antenna has radius R then the effective diameter is $2R\sqrt{\eta}$, where η is the aperture efficiency. Thus, the beam width of a circular filled aperture antenna is approximately 1.09 $\lambda/(2R\sqrt{\eta})$.

For an array, the beam width at zenith is 1.02λ/diameter, where factor of 1.02 arises if a uniform grading is used across the array. For a filled aperture antenna, there will be a taper across the aperture and this factor is approximately 1.09. Using the array radius calculated above, it is found that the ratio of beamwidth at zenith for a filled aperture and array of the same total area is:

$$\begin{aligned}\frac{\text{Beam width filled}}{\text{Beam width array}} &\approx \frac{1.09}{1.02\sqrt{\eta}}.\left[\frac{1.05}{\sin(\theta)}\right]\\ &\approx \frac{1.12}{\sin(\theta)\sqrt{\eta}}\end{aligned}$$

For the array a change in aperture efficiency does not decrease the effective radius but only the effective collecting area. Thus, there is no increase in beamwidth as occurs with a filled aperture antenna as the aperture efficiency decreases. The ratio of the beam areas is equal to the square of the above ratio.

At elevations other than zenith the array will be foreshortened and this increases the beam area by a factor equal to 1/sin(θ), foreshortening will affect the beam size in only one dimension. Assuming this increased beam area can be fully utilised and that observations take place uniformly over the sky at elevation greater than θ, then the average beam area of the array is increased by:

$$\begin{aligned}\text{Average beam area increase} &= \frac{\int_\theta^{\pi/2} \frac{\cos(\varphi)}{\sin(\varphi)}.d\varphi}{\int_\theta^{\pi/2} \cos(\varphi).d\varphi}\\ &= \frac{\ln(\sin(\theta))}{\sin(\theta)-1}\\ &\approx \sin(\theta)^{-0.45}\end{aligned}$$

The approximation is accurate to better than 2% for θ greater than 12 degrees. Combining the two equations, it is found that

$$\frac{\text{Beam area filled}}{\text{Average beam area array}} \approx \frac{1.25}{\eta \sin(\theta)^{1.55}}$$

Appendix D
Horizontal Axis Cylindrical Reflector

D.1 Mechanical construction

The design used at Molonglo provides a good starting point for the method of constructing a horizontal axis cylindrical reflector. A plan view and side elevation from the original engineering drawings is shown in the figure below [supplied by Duncan Campbell-Wilson].

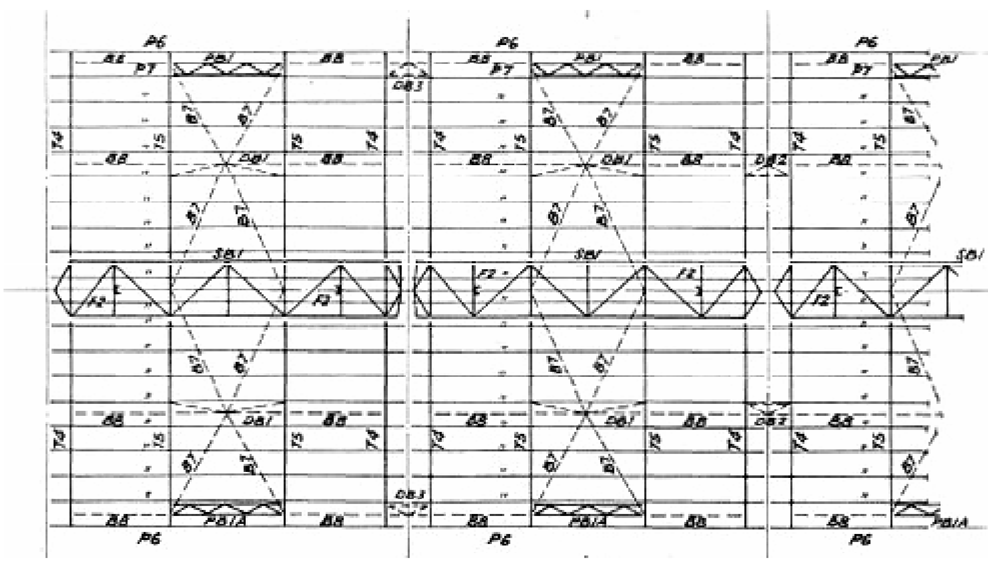

Figure 10 Plan view of Molonglo East-West arm

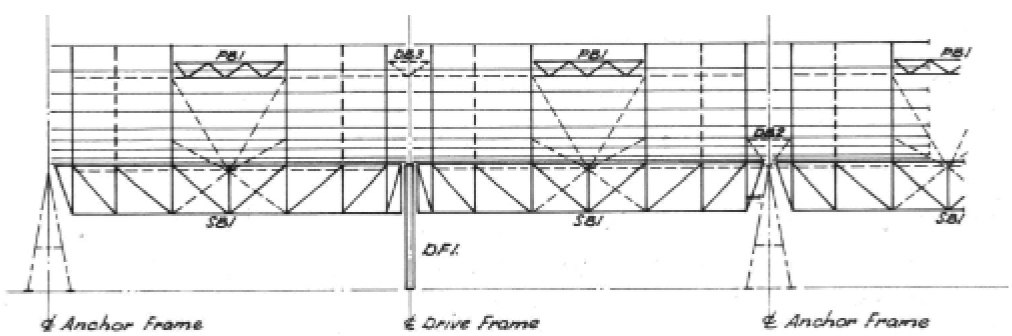

Figure 11 Side elevation view of Molonglo East-West arm

The side elevation shows that the reflector is supported on alternating drive and anchor frames. The anchor frames have no drive mechanism and provide lateral and longitudinal support. Because the drive frame must provide clearance for the sector gears, it is narrow and only provides longitudinal support. Spanning the space between the frames is a spine beam (SB1), which is supported on bearings at the frames. The spine beam is about two purlin spacings wide and is most clearly seen in the plan view. A sector gear (not shown) is attached to the drive frame end of the spine beam to rotate the spine beam and the rest of the structure supported by it. To form the parabolic surface cantilevered trusses (T4 and T5) are attached to the spine beam. An end view of the reflector at Ooty (shown below from Swarup et al. 1971) illustrates the form of these trusses for an offset fed design.

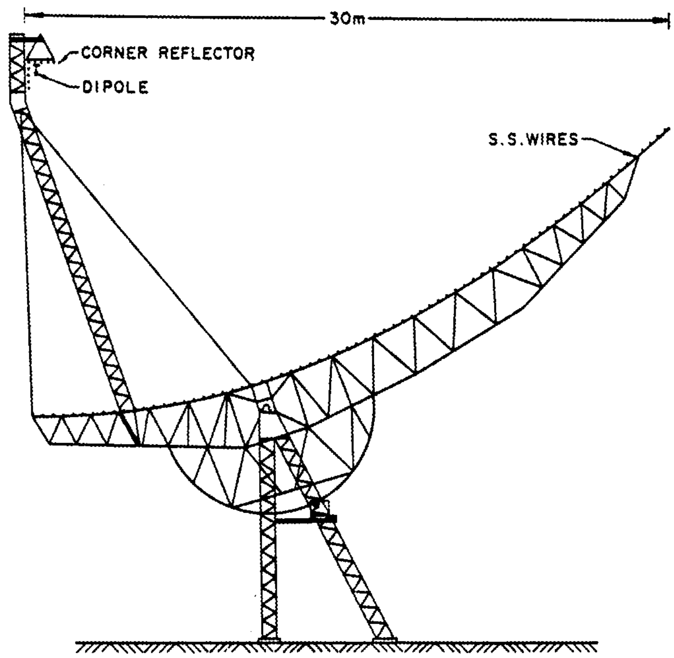

Figure 12 End view of the Ooty cylindrical reflector

At Molonglo, there are four pairs of cantilevered trusses per spine beam. Twenty purlins across the width of the reflector are welded directly to the trusses forming the basic structure of the telescope. Extra features that can be seen in Figure 10 are diagonal bracing to increase the torsional rigidity of the structure and extra beams near the ends of the cantilevered trusses. The structure is partially supported on these extra beams when it is parked.

D.1.1 Molonglo Maintenance Issues – Multiple separate units

The design at Molonglo was not conceived with minimum maintenance in mind. Duncan Campbell-Wilson, the Officer-in Charge at Molonglo, has pointed out a number maintenance issues with the current telescope. Future designs will benefit by trying to minimise these problems.

In the actual construction of the reflector tubular steel was used. Water can get trapped in the tubes and cause corrosion, and if the temperature drops below zero the water freezes and can split the tube open. In any new design the open section members should be used such as I, U and C channel beams. Other major maintenance problems involve the drive system. The drive system consists of single motor driving a shaft that runs the length of each reflector. This shaft passes through a gearbox on each drive frame, and to remove thermally induced stresses, there is a flexible coupling in the drive shaft. The flexible couplings and gearboxes are high maintenance items.

When there is mechanical drive failure part of the surface ceases to be driven. As the purlins run the full length of the reflector the failed section is kept moving by forces transmitted through the cantilever trusses to the purlins. This can cause the surface to twist which leads to time consuming realignment. At the low frequencies that Molonglo operates, the twisting and untwisting does not seem to degrade the performance of the reflector. This twist and untwisting of the structure is to be avoided because of the deformations it can cause to the surface as well as the cost of repair. As it is not possible to guarantee that there will never be any mechanical failure, the full length of the reflector should be broken up into sections, each of which is self supporting after any mechanical failure.

When broken into a number of smaller units, a separate motor can drive each section of the reflector. This eliminates the long drive shaft and its high maintenance couplings. The motors that replace the couplings can be very reliable. The main cost in using separate section is that each section needs an encoder, but it may not be necessary to put a precision encoder on each section. Then observing, the edges of each section move in unison. This can be used to servo one section off an adjacent one. At Molonglo each gearbox/drive system activates about 20m of the reflector. If this is the size of the basic unit and adjacent units are servo controlled, then only one encoder is needed for each $600m^2$ of the reflector, or three in the case of a $1670m^2$ SKA antenna station.

An example of such a servo is a modulated infrared LED on one end of a purlin for one section shining onto a pair of adjacent detectors attached to the corresponding purlin of the next section. When aligned the signal in the two detectors is equal. As the gravitational and possibly thermal deflection in the two sections will be identical, then maintaining the relative position of the two sections will maintain their relative pointing. On sections without a precision encoder some form of coarse positioning is needed to bring the servo into lock.

D.1.2 Drive options

With one drive and encoder for a 15 by 30m section there are 2200 units. Each drive unit can cost a couple of thousand dollars without exceeding cost limits. A motor and gearbox driving a sector gear is the tradition method of driving the antenna. Other options include hydraulic drive, which in the event of failure will soften the fall and reduce damage, and motorised threaded actuators, which can function as both drive and encoder. Whichever system is used, it must not compromise the reliability of the final system.

D.2 Surface

If purlins are used to define the surface, then a 60cm spacing with linear segments between purlins will reduce the reflector efficiency to 99% at 1.4GHz. Reducing the purlin spacing by a factor of three increases the maximum frequency by a factor of nine. Thus, 20cm purlin spacing allows sufficient surface accuracy to operate at frequencies beyond 12GHz. At these frequencies a fairly solid surface is needed and expanded metal mesh, or similar, would be used instead of the wire mesh currently employed at Molonglo. The rigidity of this material would allow the surface to be a better approximation of a parabola and the purlin spacing could be increased. Estimated cost of material for an expanded metal mesh surface is US$17M. A detailed analysis of the effect of purlin spacing, surface material options and alignment methods is given in [Appendix G].

D.3 Fan beam rotation with longitude

A cylindrical reflector is necessarily longer than it is wide and when fully beamformed a fan beam in generated. At long East-West baselines the axes of the reflectors at each antenna station cease to be parallel. This can lead to a rotation of the fan beams relative to each other. For sources on the celestial equator, there is no rotation but the meridian will be different for antenna at different longitudes. As the pole is approached, the fan beams from antenna stations at different longitudes rotate with respect to each other, while at the same time the meridian distance offset decreases. At the pole the relative rotation of the fan beams is equal to the difference in longitude between the antenna stations. In the worst case (a longitude difference of 90 degrees) the fan beams are orthogonal and for the 111 by 15m reflector the width of the area that can be imaged is reduced by a factor of 8 to about 8 by 8 arc minutes at 1.4GHz.

On a 10,000km baseline the resolution is about 4 milliarcsec at 1.4 GHz. With 3 pixels per resolution element, an 8 arc minute VLBI map could still have over 10^{10} pixels. However, the size of a VLBI map is limited to much less than this by delay smearing, non-isoplanatic effects and even with the SKA, insufficient independent UV data. Thus the possible reduction in beam area with VLBI baselines does not impose any limitations on the science. Indeed, the processing of one fan beam satisfies the SKA criterion for the number pixels in a map, but in generating this image only 1/8 of a eight-fan beam correlator is used. The rest of the correlator could be use to form 8 extra independent images anywhere within the 40 square degrees that are accessible at 1.4GHz by the cylindrical reflector beamformer.

Appendix E

Vertical Axis Cylindrical Reflector

John Bunton
CSIRO Telecommunications and Industrial Physics

A cylindrical reflector needs at least one axis of mechanical rotation if it is to scan most of the sky. With a horizontal axis of rotation and line feed scanning to ±60 degrees some 87% of the sky can be accessed at any one time. Mechanical limitation may reduce this to 70-80%. Full sky coverage can be achieved if a vertical axis of rotation is used with a design such as the doublet antenna proposed for the SKA by James & Parfitt [1]. The principle behind this design is the mounting of tilted cylindrical reflectors on a wheel on track rotator. This principle can be applied to any antenna technology Bunton [2] where this type of mount is described as a TiltAz mount (Tilted antenna and an Azimuth mount). The doublet antenna, figure below, is an example of a cylindrical antenna mounted in this way. Other possibilities are a centre fed cylindrical reflector (for example the AS-999A military search radar Law [3]) and dual pairs of offset fed reflectors (a double doublet?).

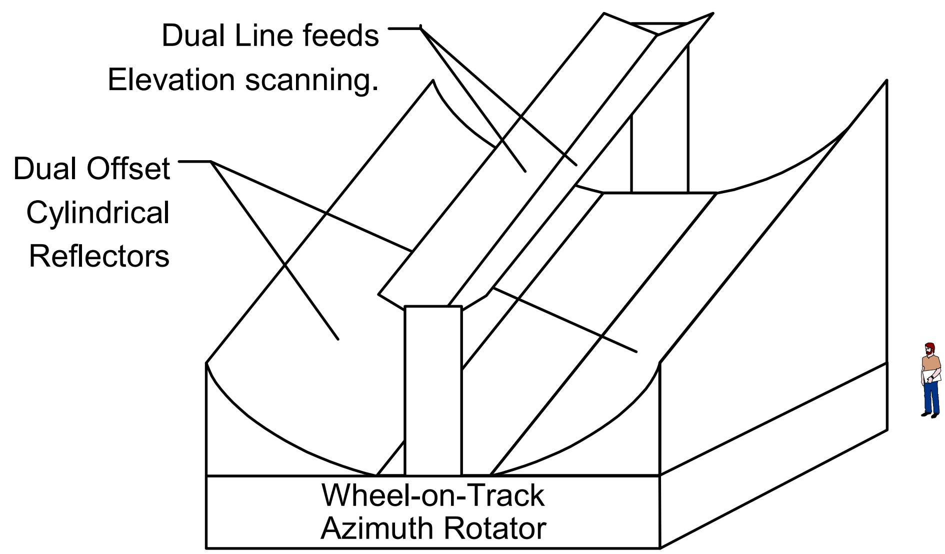

Figure 13 Doublet or dual cylindrical TiltAz antenna

Azimuth scanning is mechanical and elevation scanning is achieved electronically in the line feed. By using a 45-degree tilt on the cylindrical reflector the total electronic scanning range is reduced to ±45 degrees for full sky coverage. This reduces the maximum loss of effective area to a factor of 0.7 at the horizon and at zenith. But only 4% of the sky is within 15 degrees of zenith and almost all reflector and lens technologies have shadowing problems at low elevations. Thus, the reduction in effective area is at most 13% when scanning ±30 degrees (15 to 75 degrees elevation). This would be a more appropriate figure to uses when comparing the cylindrical TiltAz antenna to other technologies.

E.1 Selecting the Basic Antenna Topology

As with horizontal axis designs, an offset fed reflector is probably preferable because it reduces reflection off the surface and back to the line feed. However, neither centre nor offset-fed designs have an advantage when it comes to accessibility to the line feed. In both cases the line feed is difficult to access as can be seen for the case of a doublet in Figure 13. For very little extra cost the line feed can be mounted on pivoting supports so that the whole structure could be lowered to a point close to the surface of the reflector. If this were done, the offset design has the advantage that the stairs and service platforms could be built into the structure in the area directly under the line feed. This leads directly to a design such as the doublet, which uses dual offset reflectors with a common support system for the two line feeds, Figure 13.

The next important thing to decide in the design is the size and aspect ratio of the reflectors. A wheel on track mount requires that the reflector when viewed from above enclose an area that is approximately square, possibly with a length to width ratio of at most 1.4. 10m wide reflectors with a ~5m gap between reflectors give a total width of 25m. The horizontal length of the reflector can be up to 35m with a physical reflector length of 50m. The total collecting area for the antenna is 1000m^2, which would be suitable for a 1000 antenna station SKA.

The height of this antenna could be reduced if the width of the reflector is increased but this reduces the length to width ratio. This lowers aperture efficiency due to problems at the end of the reflector. If the line feed is equal in length to the reflector then as the beam is scanned electronically part of the line feed ceases to see the surface of the reflector. This can be minimised by using a short f/D ratio but cannot be eliminated. At a scanning angle of 45 degrees a length of reflector equal to the focal height is missed. Assuming an f/D of 0.3 then a 10m reflector loses about 3m in length. But worse than the loss of area is unwanted interference and noise picked up by the end 3m of line feed. The end section of the line feed needs to be turned off. In a practical design the reflector will be longer than the line feed. If the end three metres of line feed were not installed then a 35m long reflector would have a 29m line feed. This leads to a decrease in aperture efficiency of 17%. Decreasing the length of the reflector leads to increasing loss, which is unacceptable. An increase in the length of the line feed reduces the loss but introduces the complication that part of the line feed should be selectively turned off as elevation changes. There is also extra noise pickup that degrades performance.

The reduction of aperture efficiency as the reflector gets shorter and the increase in line feed cost as the reflector gets narrower leads to the conclusion that the minimum antenna size for the SKA is not much less than 1000 m^2. A larger antenna could be built by increasing the width of the reflector to 14m and maintain the proportions of the 1000 m^2 design. This gives an antenna station with 2000m^2 of collecting area. The antenna structure would be 35m across by 50m deep and 50m high. For a 3000m^2, antenna a four-reflector design, which reduces total height, becomes an option. In this case 10.5m reflectors could be used and the distance across the four reflectors including inter reflector gaps is ~50m. The ground plan is square and each reflector is 71m in length. This design, using the scaling that cost per m^2 is proportional to area$^{1.35}$, is expected to cost 46% more per antenna station than three 1000m^2 doublets. Even though the three-antenna design is cheaper to build, the single antenna has the advantage of minimising correlator cost, eliminating shadowing at low elevation, high filling factor, less loss due to end effects and only one set of mechanical components.

E.2 Construction

The design can be broken up into four parts: the foundation and track, bogies, supporting structure, reflecting surface and line feed.

E.2.1 Foundation, track and bogies

There are two approaches to designing the foundations and track. In one approach, it can be built to high precision so that there is negligible distortion and error as the antenna rotates. This could be costly if a track has to be aligned to millimetre or better precision. A simpler and cheaper approach is to build the foundations to a lower precision, say 1cm, and use either a three-bogie design or self-levelling bogies. In the three-bogie design, the axis of the antenna will move as the antenna rotates, due to errors in the track, but no significant stresses are set up in the structure due to this movement. If the error is kept to less then 1cm then the tipping of the structure with a 20m track is at most 17 arcmin. The error can then be measured with level meters. In the self-levelling approach, the supporting structure would be mounted on an interconnected hydraulic suspension similar to the hydrolastic suspension of the Morris Mini motor car. This suspension would maintain a constant vertical relative height at each bogie.

E.2.2 Supporting structure

The supporting structure locates the purlins on which the reflecting surface is mounted and supports the line feed. Its basic geometry is that of a wedge supported by the bogies. One of many possible designs uses four bogies placed at 90 degrees around the track. Main beams that overhang the bogies by about half the radius of the track connect two adjacent pairs of bogies, as is shown in Figure 14.

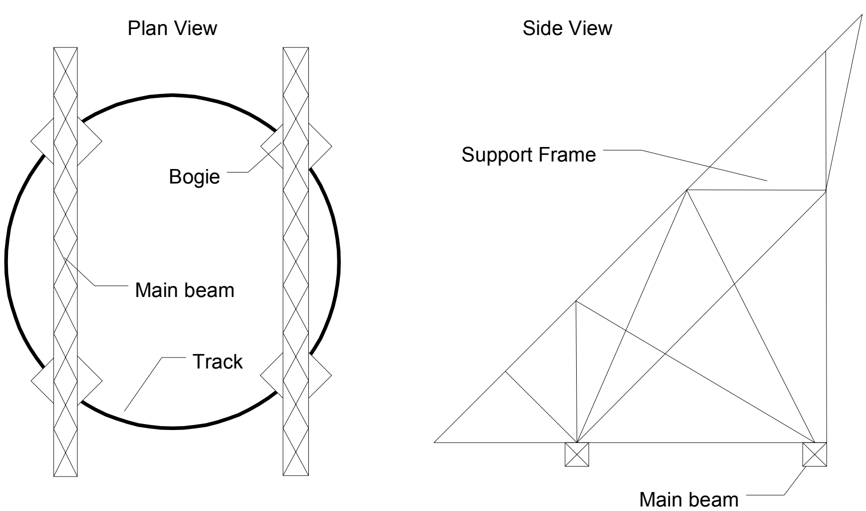

Figure 14 Possible construction for large cylindrical TiltAz antenna

The main beams are then used to support a number of support frames. At a minimum, there will be one support frame for the line feed and inner edge of the reflector and one at the outer edge of the reflector. For a four-reflector design, five support frames are needed. Cross bracing, not shown, between support frames is needed to ensure rigidity. The gap between the support frames is about 12m and is spanned by trusses at about three metre intervals. These trusses define the parabolic curvature of the reflector. Purlins running lengthwise along the reflector are attached to the trusses. It is expected that the support frame and trusses will rely heavily on construction techniques used in steel frame house and roof truss construction.

E.2.3 Reflecting surface and line feed

The reflecting structure and line feed are common to all designs and will be dealt with in the following Appendices 7 and 8. But in cylindrical TiltAz designs, access to the line feed is especially difficult. With an offset reflector the area under the line feed can be used for access but there is still the problem getting to the height of the line feed. As mentioned previously, the whole structure could be hinged at the top and bottom of the line feed supports. After freeing the hinges, the whole structure can be winched down to the level of the reflector. The alternative is to hinge the line feed supports at their halfway point. Sections of the line feed can then be rotated down to a suitable height.

[1] James, G.M. & Parfitt, A.J., 'A Low-Cost Cylindrical Reflector for the Square Kilometre Array', in Perspectives on Radio Astronomy: Technologies for Large Antenna Arrays, (eds.) Smolders & van Haarlem, ASTRON, 1999

[2] Bunton, J.D. 'TiltAz Mounted Antenna', The SKA: Defining the Future, Berkeley Workshop, July 2001 http://www.skatelescope.org/skaberkeley/

[3] Law, P.E., 'Shipboard Antennas', Second Edition ARTECH, 1986, pp265,266,352

Appendix F

Fixed Cylindrical Reflector

Stuart G. Hay and John D. Bunton
CSIRO Telecommunications and Industrial Physics

A fixed reflector solution to the SKA antenna problem has significant appeal because of the savings to be made in the construction. The feasibility of such an approach has been shown by Hay [1] where fixed dual-reflector multibeam antennas based on either paraboloidal or cylindrical reflector antennas are demonstrated. An example of a multibeam cylindrical antenna that can provide significant sky coverage is the 'Opera House antenna' shown in Figure 15. It uses an almost flat primary reflector with a large secondary reflector. Scanning over 40° is achieved by moving the line feed. This mechanical movement is expected to be considerably cheaper than moving the full reflector as in a horizontal or vertical axis design. This saving must be offset by the cost of the secondary reflector and the fact the scanning angle possible is approximately proportional to the size of the secondary reflector. However, if a system with multiple or duplicated line feeds is envisioned the design comes into its own because it gives cylindrical reflectors multibeaming flexibility approaching that of a Luneburg lens.

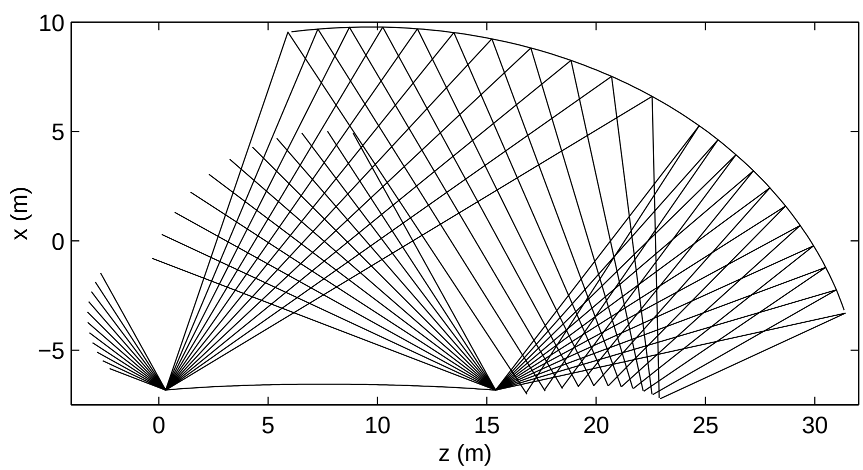

Figure 15 Cylindrical Opera House Antenna with 40° field-of-view.

At 6GHz, the radiation patterns (Figure 16) are of very good quality, indicating very small aberrations; results at 9GHz indicate that the antenna could even be operated at this frequency. This design would require a line feed with a -10dB half-beamwidth of about 24°. The loss in gain at +20° is due to foreshortening on the main reflector as the angle of view tips over towards the horizon.

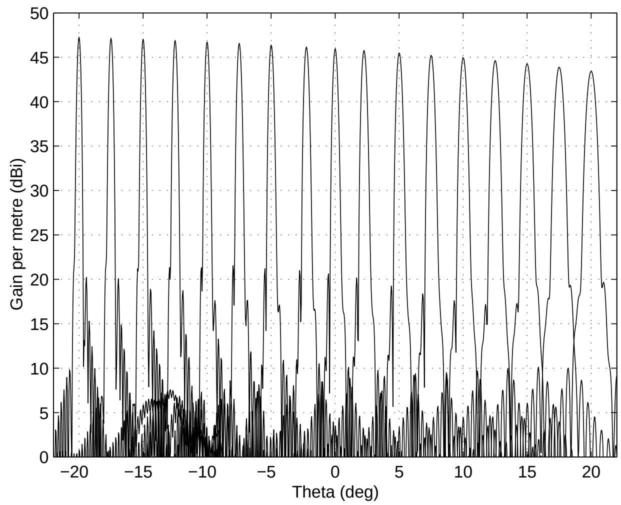

Figure 16 Radiation patterns of cylindrical Opera House Antenna at 6GHz.

If this antenna is oriented North-South it provides the sky coverage shown in Figure 17. It has good declination coverage at transit but Hour Angle coverage is limited to ~1.5 hours each side of transit. This increases to over 2 hours for declinations greater than 45 degrees.

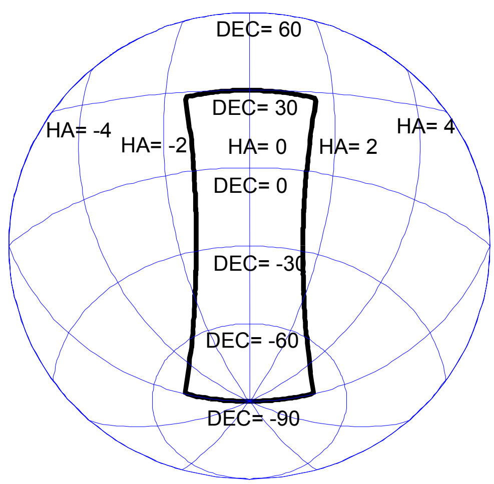

Figure 17 Sky coverage for a fixed North-South Opera House Antenna

This sky coverage is probably insufficient for SKA requirements and can be extended by using multiple fixed reflectors. An example of four Opera House antennas is shown in Figure 18.

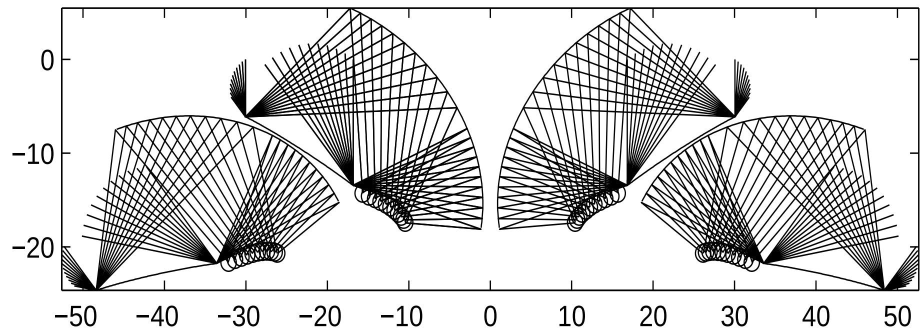

Figure 18 Cylindrical Opera House Array with a total field-of-view of 160.

With the four antennas shown, the accessible sky is now almost from horizon to horizon. Construction costs are reduced because, in most cases, backing structure can be shared between two reflectors. What is unknown at the moment is the true cost trade-offs between fixed multiple reflectors and a single moving reflector.

[1] Hay, S.G. in preparation

Appendix G

Surface construction

John Bunton
CSIRO Telecommunications and Industrial Physics

In both horizontal and vertical axis technologies the simplest method of supporting the surface is on straight support elements or purlins that run parallel to the long dimension of the cylinder. Each purlin defines one point on the parabola in the plane orthogonal to the purlin. Between the purlins the simplest method of forming the surface is to stretch metal sheet or wire mesh. This leads to a straight-line segment approximation of the parabola.

G.1 Purlin spacing

The error due the straight-line approximation is easily calculated. The maximum deviation from the nominal parabola (defined by the purlin location) occurs midway between the purlins. To calculate this error consider a nominal parabola defined by $y=x^2/4f$ (f is the focal length), with purlins placed at x=D and x=D+2d. At the midpoint between the purlins the parabolic surface is at $y=(D+d)^2/4f$ and the straight line approximation $y= [D^2 + (D+2d)^2]/8f$.

Thus the error E in y at x=D+d is: $E=d^2/4f$

It is seen that the error is independent of D but depends on the focal length f and the square of the purlin separation d. Thus halving the purlin separation quadruples the maximum possible operating frequency.

For the Molonglo reflector, f=2.9m and 2d=0.6m thus the error E=7.8mm. At the centre of the reflector the total error in path length is double this. The error varies in a parabolic fashion from zero at the purlins to 1.5cm at the midpoint. Subtracting the average error and normalising the purlin location to +1 and –1 gives the path length error E(x) in radians at a wavelength λcm of

$$E(x)= 2\pi(1.56/\lambda)* (x^2 -0.333)$$

The change in antenna gain *G* due to this error is

$$G = \frac{\int_{-1}^{1} \cos(3.12\pi(x^2 - 0.333)/\lambda)dx}{2}$$

For λ=21cm the effective gain G of the centre part of the reflector at the Molonglo reflector is 0.99. For other sections of the mesh the error is less. The very edge of the reflector is level with the feed thus a vertical displacement of the mesh does not cause any change in path length from the mesh to the feed and the total path length difference is reduced to 7.8mm. This reduces the loss in effective area to a factor of *G*=0.998.

G.2 Surface material options

At lower frequencies, the cheapest surface material is wire mesh. For example, galvanised aviary mesh with a 6.5 mm x 6.5 mm mesh size with 0.6 mm wire diameter costs[4] about US$75 for a 1.2 by 30m roll, or about US$2 per square metre. This material has good reflectivity up to a couple of Gigahetrz but has little structural rigidity. Because of this, straight-line segments between the purlins define the surface. With the 0.6m purlin spacing at Molonglo the loss in gain due to the straight line approximation is 4% at 3GHz reducing. If the purlin spacing is reduced to 0.3m, and with no other errors, a mesh surface would be useable to 12GHz. However maintaining 2mm accuracy with such a mesh would be difficult, a more rigid surface is needed.

Expanded or perforated metal sheet could also be used to form self-supporting surfaces between purlins. If the metal sheet spans a number of purlins then the rigidity of the sheet will make the surface conform to an approximately parabolic shaper, leaving mainly setting error to degrade the accuracy of the surface. Suitable expanded metal sheet costs about US$17 per square meter[5]. The advantage of this material is that access from one side of the surface only is sufficient to fix it to the purlins. The location of the purlin is clearly visible through the surface. Thus, the fixing method could use self-tapping screws placed through the holes in the mesh and drilled into the purlins. Expanded metal mesh or perforated sheets with 3mm holes should have a reflectivity suitable for operation up to12GHz.

An alternative to individual purlins is corrugated steel cladding where the edge-on shape is reminiscent of a square wave. This has sufficient rigidity to span the space between the parabolic trusses. For this application, the cladding needs to have perforations to allow rain to run off. When expanded metal sheet is attached to this backing structure the sheet and the cladding form multiple box girder structures giving the whole assembly a high degree of rigidity and strength.

G.3 Surface alignment

The size of any cylindrical reflector precludes the option of manufacturing the surface as a single piece. Thus, the surface will need to be aligned after it is assembled. This can be accomplished by attaching a template to each end to the reflector and shining lasers set on one template onto reference marks on the other. Then a simple detector sitting on the surface, or pushed through the surface, can then determine the error in relation to these reference laser beams. Thus, the setting of each point on the surface is simply a matter of adjusting the surface relative to the measurement determined by the detector. The only metrology needed is the setting of the templates. The axis of rotation determines one reference point and the final degree of freedom, rotation of the template, could be determined by installing matched tilt meters on each template. The tilt meters themselves are calibrated with the two templates bolted together.

---

[4] Obtained by Duncan Campbell-Wilson from a local supplier, volume prices should be lower

[5] Obtained by George Warr from Expamet

Appendix H

Line feed

John Bunton
CSIRO Telecommunications and Industrial Physics

For a cylindrical reflector the number of feed elements needed increases linearly with frequency. Thus, even if the cost of an individual feed element was independent of frequency the cost of the line feed will dominate at higher frequencies. With $\lambda/2$ metres spacing of feed elements at the maximum frequency, there are $2/\lambda$ feed elements per m. For a reflector width of *w,* the total length of length of the cylindrical reflectors is 1,000,000/*w* for one square kilometre SKA. The total number of feed elements is equal to this length times the number of elements per metre:
2,000,000/(λ * width of reflector). For a reflector 15m wide operating at a maximum frequency of 3GHz (λ = 0.1m) the number of feed elements needed is 1.33 million rising to 2.67 million at 6GHz. End effects will reduce this number by about 10%.

To maximise the upper frequency of operation it is necessary to minimise the cost of the line feed and, in particular, the LNAs. The actual feed gets smaller with frequency and there may be some saving, but for the same performance LNA costs always increase with frequency and it is the LNA cost that will eventually dominate.

H.1 Feed elements

The actual feed elements that the line feed is made out of represents one of the greatest areas of uncertainty in the design of a cylindrical antenna for the SKA. All other areas have known solutions, with the limiting factor being cost. This is not true for the feed, which may need to cover a frequency range of 0.1 to 12GHz. A single feed element cannot cover this 120:1 frequency range. To cover this range with a minimum number of line feeds, each feed needs to cover as great a frequency range as possible.

One possibility for a wideband feed is a log periodic such as that designed for the ATA, which can cover a 20:1 bandwidth. This feed is suitable for antenna with medium to long f/D and would need mechanical steering. Among other problems, the feed width is about 5λ making difficult to eliminate grating lobes. Some other the options are crossed bowtie, rabbits ear and Vivaldi feed elements. Work within the SKAMP projected is aimed at solving this problem

H.2 LNAs

If an upper frequency limit of 9GHz is specified then the total number of LNAs with dual polarisation is ~7 million (assuming the LNAs are directly connected to the feed elements). For a viable SKA the cost of an LNA needs to be less than about US$10. This precludes the use of cooling and makes unattainable the ~3 times reduction in LNA noise temperature that cooling to liquid nitrogen temperatures can give. But, in addition to the LNA noise, there are other noise contributions such as those from the microwave and galactic backgrounds, atmospheric emission, losses in the feed and matching network, and spillover. These other sources of noise contribute at least 15K to the system temperature at 1.4GHz. At low elevations, low galactic latitudes and at frequencies above 10GHz and below 800MHz, these contributions to the system temperature are even higher. Once uncooled LNA noise temperatures approach this limit, the total difference between cooled an uncooled systems becomes much less. For example, an uncooled HEMT design for the Molonglo radiotelescope being developed by Ralph Davidson has achieved a 20K or better noise temperature over the frequency range 300MHz to 1.2GHz. Thus if other factor add 15K the total system temperature will be 35K as compared to an estimated 22K if the LNA were cooled. The uncooled system is only 60% worse.

Although currently not providing as good a noise performance, SiGe HBTs may eventually provide the cheapest solution as the bare transistor has close to 50Ω input and output match leading to a much simpler design and alignment. One of the best devices currently available is the BFP620 from Infineon (US$ 0.3 in quantity), which has a published performance of 44K at 0.9GHz, 50K at 1.8GHz, 70K at 3GHz and 100K at 6GHz. This device is already ideally suited to use as the second stage amplifier in an LNA, and if used in the Ralph Davidson design it significantly reduces costs.
If it is assumed that devices improve at 15% per year, as is seen for the sample of LNAs in Figure 8 Appendix B, then by the time the SKA is being built the 6GHz performance of a SiGe transistor will be about 25K. Such a device would make cooling unnecessary at 1.4GHz and greatly reduce the advantage of cooling at 6GHz. That this is possible is shown by the research device built by IBM Niu & Zhang [1] with a spot noise temperature of 14K at 2GHz (2:1 bandwidth noise temperature should be close to this as the bare device is close to a 50 ohm match by itself). This device already achieves the extrapolated 2010 performance of the BFP620-like device. Extrapolating from the results for the research device indicates that a 7K device may be available for the SKA at 6GHz. Such a device would render the need for cooling unnecessary at frequencies up to 10GHz and result in an LNA cost of about US$1.

H.3 System Temperature

It is hard to estimate the noise temperature attainable with uncooled devices in 2010 but hopefully it will be possible to replicate the results of Niu and Zhang and have an LNA with a noise temperature of 14K. In Appendix K it is estimated that spillover will contribute 3.5K. Add to this 3K for the cosmic microwave background, 3K for the sky, 2K for calibration and 4.5K in feed losses and the Tsys that should be achievable is 30K.

H.4 RF Beamformer

For every feed element, there must be an input to a beamformer. In early designs with full sky coverage, a mechanical approach has been taken: rotating helices or feeds at Molonglo and moving plungers at Ooty. Mechanical systems will be too costly to build and maintain for the SKA. Thus, electronic beamforming must be used. The final stage of beamforming in all designs will be digital, but it is too expensive to digitise at each feed in a cylindrical reflector. An extra constraint on the SKA is that the system is broadband, and between the feed and the digitiser a true delay beamformer is needed; phase shifters will not provide enough bandwidth. The beamforming can be done either at RF or IF. RF beamforming has the advantage that it minimises the number of filters and down converters. Thus, this strawman design uses a first level of RF delay line beamforming followed by digital beamforming.

Cost can be brought to an absolute minimum if the RF beamformer were to be connected directly to the feeds. This could reduce the number of LNAs by a factor equal to the number of inputs into the RF beamformer. This is done currently on existing cylindrical reflectors, with beamformer losses ranging from about 1dB down to 0.2dB at frequencies below 1GHz. These losses are comparable to loss in broadband power combiners and, when the losses due to switching are added, it is probable that the RF beamformer will add 20K to 100K to the system temperature. This degree of degradation is unacceptable in designs where the total system temperature is hoped to be less than 50K today and about 20K by the time of the SKA. Thus, it is desirable that the design use LNAs ahead of the RF beamformer. This is now a possibility because, as has been shown in the previous section, the LNA cost should be low enough. The time-delay RF beamformer itself is now becoming economic with the introduction of MEMs and Silicon-on-Insulator (SOI) switches. In volume the SOI switch will cost as little as 30cents each [2], however MEM switches promise the lowest loss. The use of these switches in mobile wireless communications will continue to drive down costs, improve performance and in the case of MEM improve durability.

One limiting factor of the beamformer design is the number of inputs into the digital beamformer. This limits the instantaneous sky coverage of the cylindrical reflector. Assume there are N feed elements, spaced at $\lambda/2$ per digital input. The field-of-view of the signal at the input is ~2/N radians at the highest frequency of operation of the line feed. This situation is not improved by forming multiple beams in the RF beamformer. For example, if two RF beams are formed, then each digital input must operate on the sum of signals from 2N feeds. There are twice as many RF beams but each has half the beam width so the sum total of the field-of-view is unchanged. After digitising the cost of beamforming is low and with Moore's Law it will continue to get cheaper. This will allow multiple independent digital beams that do not limit the overall system.

Historical trends can help in determining the possible field-of-view at 1.4GHz for the SKA. In 1981 the Molonglo radiotelescope RF beamformed an 8.8m module of ~50 feeds. The SKA demonstrator to be built in ~2004 will RF beamform over a 1m module of 9 feeds. By the time of the SKA, 2012, RF beamforming should occur in 0.3m modules each with ~4 feeds. This corresponds to a line feed beamwidth of 28 degrees at 2GHz or 40 degrees at 1.4 GHz. The expected 1.4GHz field-of-view is 40 square degrees.

H.5 Digital beamformer

After RF beamforming the signal is converted to baseband and digitised. These signals are digitally beamformed over 10 to 15m sections of the line feed. Thus, each output from this first stage of digital beamforming corresponds to an antenna with an approximately square aperture of 150m^2 to 200m^2. To form this aperture, 30 to 50 digital signals must be delayed, fringe stopped and added. Bulk delay is easily implemented in digital delay lines. For fine delay it is proposed that polyphase filters be used. The prototype for this filter is a lowpass filter designed with a sample rate N times higher than the A/D converter rate. This is then decimated by N to give a lowpass filter. By varying the location of the first sample in the decimation the filter can be used to implement a variable delay. The compromise to be made in this design is the number of taps in the filter and the filter quality. It is expected that 10-20% of the bandwidth available at the A/D output will be lost in this process if short ~10 tap filters are used. The delayed data is then fringe stopped, and assuming complex data, this requires 4 multiplies (which can be implemented in 3). The compute load for the beamformed section is about 400 multiply accumulates. This is currently possible in two FPGAs for a 250MHz bandwidth (8-bit multiplies in an Altera EP1S120). In 10 years time, assuming Moore's Law, a single FPGA costing about US$1000 should be sufficient to provide beamforming for 2GHz bandwidth over a 12m length of line feed.

[1] Niu, G. & Zhang, S. 'Noise Modeling and SiGe Profile Design Tradeoffs for RF Applications', IEEE Trans on Electron Devices, **47**(11), p 2037, Nov 2000
[2] private communication Peregrine Semiconductor]

Appendix I

System cost estimates

John Bunton
CSIRO Telecommunications and Industrial Physics

For a reflector capable of operating to a frequency of 1GHz it is estimated that a Molonglo-style cylindrical reflector cost is US$10.9k for a 100m^2 element. To scale the cost to a higher frequency it is estimated that this cost must be multiplied to frequency f in GHz raised to power 0.333. The reflector width for the 100m^2 reflector is 11.3m. If both the width and length of the antenna were increased w metres the cost is estimated to increase by $(w/11.3)^{2.7}$. For an area of 100m^2 area of the reflector the cost increase is $(w/11.3)^{0.7}$. Thus the reflector cost is estimated to be

Reflector cost = US$10.9k * (area of SKA(m^2)/100) * $f^{0.333}$ * $(w/11.3)^{0.7}$

Costing for the line feed represent one of the greatest areas of uncertainty but using initial costing for SKAMP it is estimate that a 0.5 to 1GHz line feed will be US$230 per metre including uncooled SiGe LNAs and an RF beamformer based on Silicon-on-Insulator switches. The cost of this line feed may not decrease significantly with time, however the performance will improve. The cost is directly proportional to the maximum frequency in GHz and for wideband frequency coverage the cost of the line feed doubles if 2:1 bandwidth feeds are used. If a line feed with frequency coverage of 3:1 can be built then the total cost decreases by 25%. The total length of the line feed required for an 11.3m wide reflector is 88.5km. End effects reduce this length by about 10% to around 80km. The length also reduces as the width of the reflector increases. Thus, the total line feed cost is estimated to be

Line feed cost =US$230* 2 * f * 80,000 * (11.3/w)

After RF beamforming the signal is down converted and digitised. Costing the conversion from RF to baseband is difficult to estimate. If it were done with current conventional technology then the cost is high. However, the continuing integration of wireless frontends for mobile communication is driving the cost of integrated systems down. As an example, the Radiata RF5 and Atheros AR5111 chip are built on a standard silicon process an provides a complete 5GHz downconversion system of 20MHz bandwidth and 700MHz tunning range on a single chip. In other CMOS designs bandwidths of up to 1GHz have been achieved. Thus current CMOS processes are capable of meeting SKA requirements. Existing designs include transmit and receive, so using all the resources for receive and assuming an improvement at half the rate of Moore's Law allows up to 16 systems to fit on a single US$10 chip in 2010. Thus a dual polarisation down conversion system with one every 0.3m could cost as little as US$3.8 per GHz per metre of dual-polarisation line feed. With a three frequency-band system, this increases to US$11.4 per GHz per metre of line feed. The digitiser is expected to be more expensive. One of the best in terms of price/performance is the Maxim MAX105, which costs US$36 for a dual 6-bit converter operating at 800MS/s with a 400MHz bandwidth. In 2010, it is estimated that the performance, for equal price, will double.

With the system requiring about 1.2GHz of bandwidth for each GHz of bandwidth at the output of the beamformer three chips will be required per GHz of dual polarisation RF beamformer output. With a digitiser required every 0.3m the conversion cost is US$360 /GHz/m. The manufactured system including downconvereters is estimated to be double this cost. As the bandwidth to be process is (0.5 + *f*/5)GHz, *f* = maximum frequency, the cost is estimated to be

Downconverter/digitiser cost = US$ 743 *(0.5 + *f*/5) * 80,000 * (11.3/*w*)

Incorporating the digitiser within the downconversion chip, which is already possible, could lower cost by an order of magnitude.

In the proposed design there is digitiser for every 0.3m of line feed. For beamforming it is assumed that a ten-tap polyphase delay filter and a complex-multiply fringe stopper is used. For each GHz of bandwidth there are 20G multiplies/s in the filter and 4G multiplies/s in the fringe stopper for each digitiser. With dual polarisation, there are 160G multiplies/s per GHz per metre of line feed. With about 16 slices per 8-bit multiply, and using half the chip for multipliers, then a XC2V3000 can perform about (7000slices/16) * (1GHz/200MHz) = 88G multiplies/s. The current cost of this part is ~US$1000 and with Moores law this decreases to US$25 in 2010. Thus the cost of FPGAs for a digital beamformer is estimated at US$40 /GHz/m. Adding boards, connectors and assembly will increase this to about US$80 /GHz/m. The short baseline antennas generate eight beams falling to one for VLBI baselines. With and average of six beams per antenna a dual-polarisation digital beamformer is estimated to cost

Digital beamformer cost = US$ 80 * 6 *(0.5 + *f*/5) * 80,000 * (11.3/*w*)

Using an ASIC instead of FPGAs could lower this cost.

The digital beamformer forms beams over sections of line feed approximately equal to the width of the reflector. The number of sections is proportional to the width^{-2} because length of line feed beam formed is proportional to width while the total length of line feed is proportional to width^{-1}. For example, a doubling of the reflector width halves the length of the line feed and double the length of line feed that is beamformed. Thus, the number of beams generated decreases by a factor of four. The total number of beam formed sections equals the total line feed length divided by the length of line feed that is beamformed (w/1.2).
Total number of beam formed sections = [80,000*(11.3/w)]* [1.2/w].

Each beamformed section generates an average of six beams on two polarisations with a bandwidth of (f/5 + 0.5) GHz. A filterbank is needed for each section and the estimated cost of a 1GHz filter bank is US$3,500, which is calculated on the assumption that each input sample requires the equivalent of 24 multiplies. Using a US$200 Xilinx XC2V500 a one-Gsample/s 16-bit multiplier cost approximately US$200*6/32=US$37. With two samples per Hertz and doubling cost for other parts, manufacturing and testing gives a final cost of US$3,500 per GHz. Thus the 2010 cost of a 1GHz filterbank is estimated to be US$3500/40 = US$88. Thus, the cost of filterbanks is estimated at:

Filterbank cost = US$88 *12 * (0.5 + *f*/5) * 80,000 * (11.3*1.2/*w*^{2})

The number of correlation is dependent on the number of sections beamformed: $80000*(11.3*1.2/w^2)$. For a full Stokes correlator, the number of correlations is twice the square of the number of sections. Estimated cost of a correlation is US$16 per GHz, which is based on 25 cross-multiply units in a Xilinx XCS300E costing US$50. Assuming Moores Law this falls to 40c by 2010. Boards, manufacture, connectors etc will probably double this. Thus the cross-multiply part of the correlator is estimated to cost

Correlator cost = US$0.8 * 2 * (0.5 + *f*/5) * (80000 (11.3*1.2/*w*^{2}))^2
Again, an ASIC implementation could lower costs significantly.

The major cost of cabling is the trenching, which for Australian rural conditions, is US$10-15k per kilometre. Cable trenching in rural areas could be even cheaper than this. With six-arm example given in Appendix J, 12,000km to 15,000km of cable needs to be laid. Exchanging SKA capacity for fibre on other networks might reduce this to about 10,000km. Thus, using a median cost of US$12.5km gives an estimated cost for cabling of US$125M. All non-continental VLBI will be via recorded hard disk or will use existing fibre if possible.

Cable and trenching cost = US$125M

The total data rate for a single beam is (f/5 +0.5)GHz by 8 bits per GHz assuming 4+4bit complex data. The total data rate must be multiplied by the number of beams (8), the number of polarisations and the number of antenna sections beamformed $80000*(11.3*1.2/w^2)$.

Total data transport

$$= 80000*(11.3*1.2/w^2) * 8 \text{ bits} * 8\text{beams} * 2 \text{ polarisations} *(f/5 +0.5) \text{ Gbits/sec}$$
$$= 10{,}240*(11.3*1.2/w^2) * (f/5 +0.5) \text{ Tbits/s}$$

For a 10GHz maximum frequency SKA using 15m antennas, this is a total data rate of 1,543 Tbits/s or 2.6 Tbits/s/antenna for 8 one-degree beams. Most of this data is transported over distances less than 10km. Cheaper VCSEL devices are useable for about 60% of the data. Current cost of this technology is about US$100 per Gbit/s for the electronic-optical interfaces. This could fall by a factor of 16 to US$6.3k per Tbit/s by 2010. The maximum bandwidth is doubling every year and cost halving every two years [1]

Beyond a distance of 10km more expensive laser diodes and modulators such as $LiNbO_3$ will be needed. These cost about US$10k for a 40Gbit/s connection, but the technology does not decrease in cost as rapidly as VCSELs. At best, it is estimated, a factor of four reduction in price by 2010 giving a cost of US$63k per Tbit/s to connect the outer stations. However the data rate of outer stations is reduced as distance is increased from 10 to 3150km. If there were no reduction in the data rate these outer stations would account for 40% of the data. This is reduced to 15% of the full eight-beam data transport given above data. Stations beyond 3000km will have to rely on existing infrastructure at probably even lower bandwidths. Thus the cost of modulating the data onto the fibre and receiving the data is

Fibre TX/RX cost = 10240*(0.6 * US$6.3k + 0.15*US$63k) *(11.3*1.2/w^2) * (f/5 +0.5)
= US$135 M * (11.3*1.2/$w^2$) * ($f$/5 +0.5)

Added to this cost are optical amplifiers, with one required about every 100km of fibre. The current cost of an amplifier is US$12k and this should reduce to less than US$6k by 2010. If each station beyond 100k has on average four fibres, then there are ~400,000km of fibre. With an amplifier every 100km cost of amplifiers is 4000*US$6k = US$24M. Thus, fibre optics cost, less cable, for an SKA with an average of 6 independent one-degree beams at each antenna station is

Fibre optics cost = US$135M * (11.3*1.2/$w^2$) * ($f$/5 +0.5) + US$24M

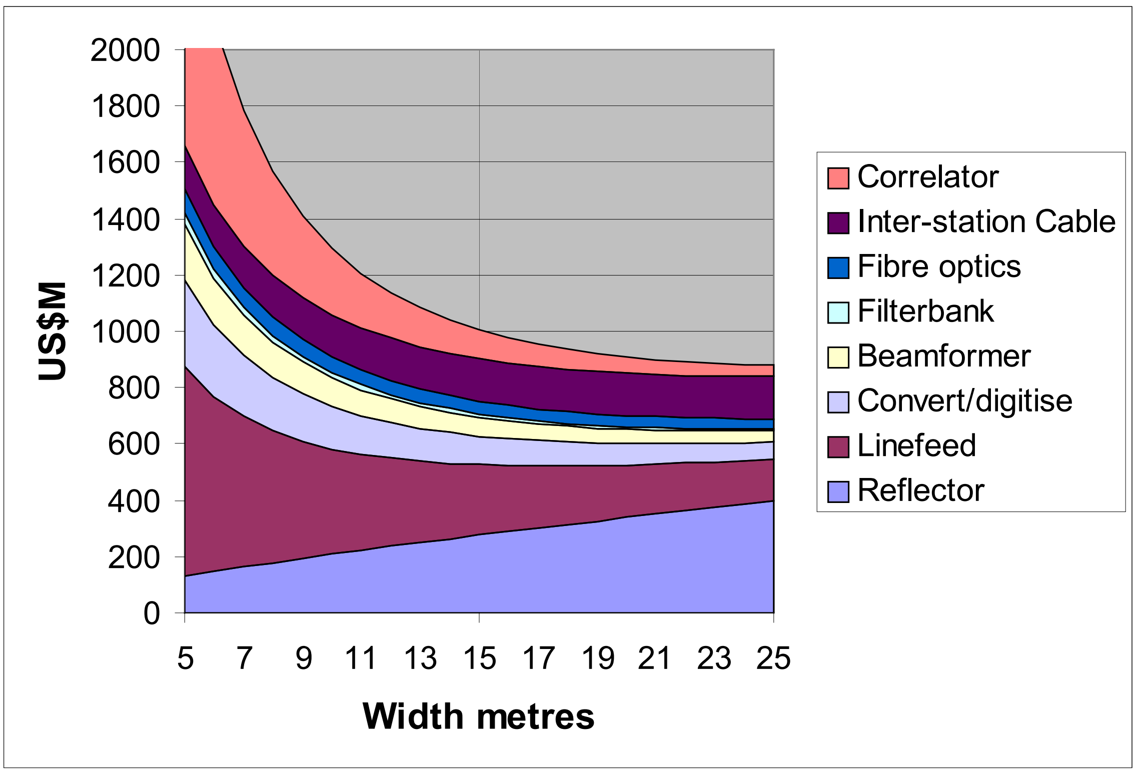

Figure 19 Cost of a 9GHz cylindrical reflector SKA with an average of six one-degree beams per antenna station.

A plot of cost versus reflector width is shown in the above figure. This is for a telescope operating up to 9GHz with a reflector good to the same frequency. It is seen that the savings in reflector cost, as the width is decreased, is effectively cancelled by the increased line feed cost. Adding the cost of digitisers, beamformers, filterbanks, fibre optics and the correlator results in a minimum cost with the widest reflector that gives a one-square-degree beam: 15m. Estimated cost of the various parts of the SKA for a number of different frequencies is given in the table below.

Table 6 Cost in US$M of a 15m cylindrical reflector SKA with an average of six beams per antenna section as a function of maximum frequency.

Frequency limit GHz	6	9	12	15	18	21	24
Processed BW GHz	1.7	2.3	2.9	3.5	4.1	4.7	5.3
Reflector	241.5	276.4	304.2	327.7	348.3	366.6	383.3
Linefeed	166.3	249.5	332.7	415.8	499.0	582.2	665.3
Downconvert & A/D	75.2	101.7	128.3	154.8	181.4	207.9	234.4
Digital beamformer	49.2	66.5	83.9	101.2	118.6	136.0	153.3
Filterbank	9.6	13.0	16.3	19.7	23.1	26.5	29.8
Correlator	77.4	104.7	132.0	159.3	186.6	213.9	241.2
Fibre-Optic cable	150.0	150.0	150.0	150.0	150.0	150.0	150.0
Fibre Interface	39.4	44.8	50.2	55.6	61.1	66.5	71.9
Full system	809	1007	1198	1384	1568	1750	1929
Reflector, Line feed and Fibre-Optic cable	558	676	787	894	997	1099	1199

These costs can be broken down into three components:

1. Those that are fixed for a given maximum frequency of operation: the reflector, line feed and fibre optic cabling cost. These are shown in the last line of the table. Note, the variation with maximum frequency is approximately US36M per GHz.
2. Those dependent only on the bandwidth processed: down conversion, digitiser and correlator cost. This cost is US$88M per GHz of processed bandwidth.
3. Those that depend on the bandwidth processed and the average number of independent one-degree beams generated. This cost is US$7.4M per GHz for one beam.

Thus if the processed bandwidth is *BW* in GHz, the maximum operating frequency is *f* GHz and the number of one-degree beams *b,* then the cost of a telescope operating to a given frequency is given by:

Cost of SKA = Fixed cost from table + 90 ****BW* **+ 9.6****BW*b*** **US$M**
~ 1000 + (*f* – 18)*36 + 90 ****BW* **+ 9.6****BW*b*** **US$M**

If the BW is equal to 0.5 + *f/5* the cost of a 15m cylindrical reflector SKA can be approximated by:

Cost of SKA ~ 400 + *f x (54 + 2 x b)* + 4.8 *x b* US$M

For a one billion dollar cost a 9GHz SKA could have a bandwidth of 2.2GHz with an average of six beams per antenna.

I.1 Cost against time

The assumptions made in calculating the above costs were that Moore's law would hold for digital based technology used in the correlator, filterbanks, beamformers and radio-on-a-chip downconverters. For A/Ds and LNAs it was assumed cost would not change but that performance would double; and for fibre optics the cost of short-range devices would halve every two years, long range devices every four years and optical amplifiers ever eight years. The effect of these scaling factors for the years 2002 to 2010 are shown below for a 15m 9GHz instrument.

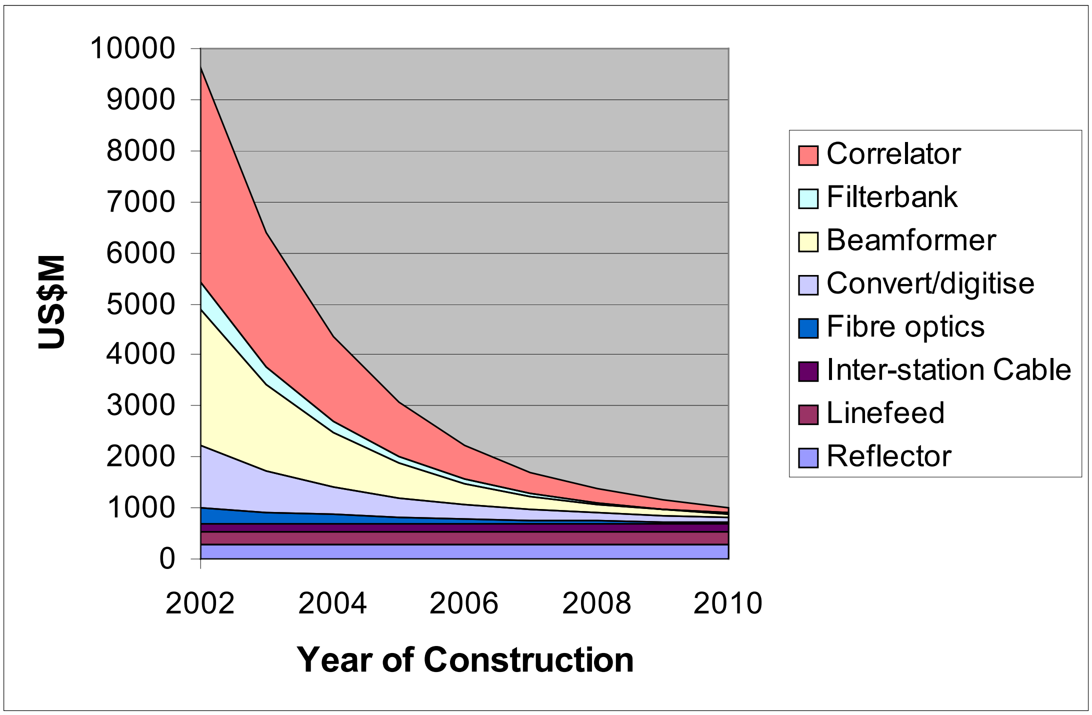

Figure 20 Scaling of costs over the next eight years

Reference

[1] http://www.nacsa.com/events/nacsaYanSun.PDF

Appendix J

SKA Siting and Array Configuration

John Bunton
CSIRO Telecommunications and Industrial Physics

The optimum latitude for the SKA is between 20 and 30 degrees. At latitudes less than this, the site gets too close to the geomagnetic equator. For sites further from the equator than 30 degrees about 1% of the sky is lost from view for each extra degree of latitude. Within Australia almost the entire landmass is in these latitudes and has a low population density and benign RF environment. Initial candidate sites have been identified in the states of Western Australia, South Australia, New South Wales and Queensland.

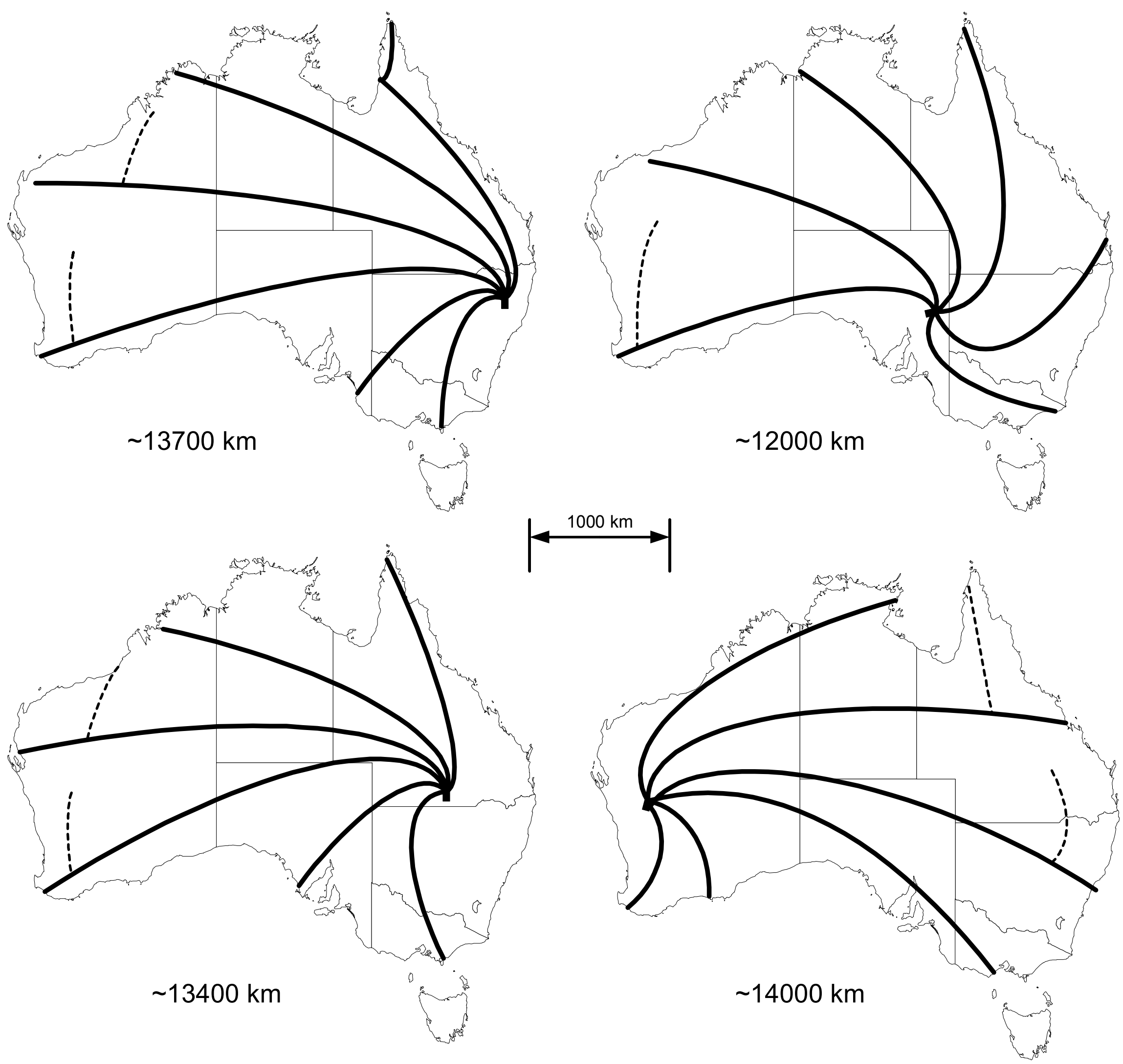

Figure 21 Four possible SKA sites in Australia showing cable routes for a 6 arm spiral VLBI network. Total length of cable indicated under map, excludes spurs.

Four examples of possible sites are shown in the above figure together with cables routes for real-time VLBI. The total length of cable ranges from 12,000km for the South Australian site to 14,000km for the West Australian site. Note that a very loose spiral has been used in these examples to minimise the cable length. See the Luneburg lens proposal for an example of a tighter spiral and further details on a possible Western Australian site.

All the configurations provide east-west baselines of 3000km or more. In the North-South direction, the maximum baselines are 2800km. Much of the sensitivity for these VLBI baselines is from correlations between the VLBI antenna and the central core. With the six-arm configuration, about two hours of observing are needed to rotate one arm onto the other at high declinations. For observation near the celestial equator, the overlap of the coverage of the arms is difficult to achieve, especially on east-west baselines. To solve this problem the ad hoc addition of north-south spurs should be considered, such as the ones shown with dotted lines in the above figure. These add about 1000km to the cable length. The added spurs, together with multi-frequency synthesis, provide a reasonable fill of the UV plane, even in snapshot mode for equatorial sources.

Considering the sites themselves, the Western Australian site has the greatest cabling cost but has the best set of east-west VLBI baselines. The most eastern site in New South Wales also has very long east-west baselines, but not as many as the Western Australian site. In a north-south direction, the coverage is very good up to 1000km. Beyond this, increasing reliance is place on lower sensitivity correlations between VLBI antennas. The Queensland site shown is similar, but with the maximum east-west baseline reduced by 400km. The South Australian site is the most central and provides excellent coverage of baselines up to 2000km. Beyond this, there is a sharp drop in sensitivity as only correlations between VLBI antennas are available.

Appendix K

Aperture Efficiency and Spillover

John Bunton
CSIRO Telecommunications and Industrial Physics

The aperture efficiency of long cylindrical reflectors can be 10% greater than that of a comparable parabolic dish. An example of this is given by Nash [1] where a parabolic grading across the aperture is considered. For the case where the grading goes to zero at the edge of the antenna the aperture efficiency is 0.84% for a cylindrical reflector and 0.75% for the circular aperture of a parabolic dish. For a taper that falls to 0.25 at the edge of the reflector, the aperture efficiencies are 0.92% and 0.85% respectively. These efficiencies are rather high to obtain more data a program has been written to calculate the aperture efficiencies for a cosine square taper. For the same illumination aperture efficiencies for parabolic and cylindrical reflectors are

Table 7 Aperture efficiency for cosine squared taper

Parabolic	Cylindrical
.85	.9
.75	.83
.65	.76

It is seen that the first two results are in good agreement with the results given by Nash. This allows the comparison to made a more realistic parabolic reflector aperture efficiency of 0.65. For the cylindrical reflector the corresponding aperture efficiency is 0.76.

The increase in aperture efficiency can be understood by considering 15m cylindrical and parabolic reflectors with the same illumination grading. For a feed illuminating the paraboloid the illuminations falls off in all directions away from the centre. Near the centre of the dish the illumination is highest but a 1cm ring at a 1m radius has an area of $0.06m^2$. At a radius of say 10m, the same ring has an area of $6m^2$ but the illuminations may have fallen to half its centre value. For the cylindrical reflector a 1cm by 6m strip has the same area as the 1m radius ring but at 10m the area of the equivalent strip has not changed, it is still 1cm by 6m. Thus, the relative amount of area affected by the lower illumination at 10m is less in the cylindrical reflector, hence the higher aperture efficiency.

Another way of looking at this is that with a line feed the cylindrical antenna has uniform illumination along its length and a grading in only across the reflector. The paraboloid has a grading in both directions leading to the lower aperture efficiency.

The spillover of the cylindrical reflector is also lower. Consider an individual element of the line feed. For a prime focus feed and the antenna pointing at zenith, it will see the ground on both sides of the reflector but will have no ground pick up for directions along the antenna. For the paraboloid, the feed sees the ground over the edge of the reflector in all directions. Thus, the ground pick up for identically configured feeds is lower for cylindrical reflectors. For the case where the illumination taper is cosine squared it is estimated that the spillover for the cylindrical reflector is about 35% of that for a paraboloid. For an aperture efficiency of 76%, the spillover is estimated at 1.2%. This adds 3.5K to Tsys.

K.1 End effects

In practice, a cylindrical reflector has a finite length. If the line feed is not to illuminate the ground directly then the line feed must be shorter than the reflector by a factor equal to the height of the feed above the reflector multiplied by tan(maximum scanning angle). Thus if the maximum scanning angle is 60 degrees, the line feed should be shortened at each end by 1.73 x width of reflector x f/D. For an f/D ratio of 0.333 the length should be reduced by 0.57 x width of the reflector. This reduces the length of line feed for the 15m x 111m reflector by 17m, which is equivalent to reducing the aperture efficiency by 15%. Such a reduction is excessive. A compromise is to design the line feed to work fully over scanning angle of 45 degrees from the meridian. In this case, the end 5m of line feed is deleted and the aperture efficiency is reduced by 9%. This gives the 15m x 111m reflector aperture efficiency reduced from 76% to 69%. Beyond a scanning angle of 45 degrees, either turn off that part of the line feed illuminating the ground, or, where one-degree beams are formed, do not use the corrupted beam. This last approach gives an extra 12% loss at scanning angle greater than 45 degrees.

K.2 References

[1] Nash, R.T., 'Beam Efficiency Limitations of Large Antennas,' IEEE Trans. Ants Prop., AP-12, pp 918-923, Dec 1964

Appendix L

Compliance Table

Parameter	Design Goal	Falls Short	Meets	Exceeds
A_{eff}/T_{sys} 0.1 GHz 0.3 GHz 1.4 GHz 5.0 GHz 9.0 GHz	**2.0×10^4 m^2.K^{-1}**		meets meets 2.0×10^4 m^2.K^{-1} 2.0×10^4 m^2.K^{-1}	With Multibeam gain 5.6×10^4 m^2.K^{-1} 5.6×10^4 m^2.K^{-1}
Total Frequency Range	**Lower 0.3 Ghz** **Upper 20 GHz**	9 GHz		0.1 GHz
Imaging Field-of-View 1.4 GHz (300 km array) 1.4 GHz (central array)	**1 deg^2** **1 deg^2**		1 deg^2 1 deg^2	2 deg^2 survey 8 deg^2 survey
Number of Instantaneous Pencil Beams	**100**	64 each 1^o x 0.12^o within 40^o x 1^o at 1.4 GHz per reflector		Multibeaming with central 1-30km antennas
Max. Primary Beam Sep.: Low Freq. 100MHz High Freq. 1.4 GHz	**100^o** **1^o**		120^o x 14^o	40^o x 1^o
Number of Spatial Pixels	**10^8 snapshot** **10^8 1 hour int.**		>100km array >10km array	>300km array
Angular Resolution 1.4 GHz	**0.1 arcsec**			0.018 arcsec
Surface Brightness Sensitivity @ 1.4 GHz (8hrs integration, 800 MHz BW) 0.1 arcsec (300km array) 13 arcsec (central array)	**1 K**			0.7 K### 0.3 mK###
Instantaneous Bandwidth	**0.5 +ν/5 GHz**		2.4 GHz	
No. of Spectral Channels	**10^4**			8192 continuum 10^5 spectral line
No. of Simultaneous Freq. Bands	**2**			3
Clean Beam Dynamic Range	**10^6**		10^6 1 hour int.	
Polarisation Purity	**-40 dB**	?	?	?
Cost	**10^9 USD**		10^9 USD	

Appendix M

Array Configuration to 31km

John Bunton
CSIRO Telecommunications and Industrial Physics

For equal sensitivity at each resolution the number of antenna within a given baseline ranges is

Table 8 Number of antenna in each baseline range.

Max Baseline (km)	1	3.15	10	31.5	100	315	1000	3150	10000
No of antennas	234	305	362	411	455	495	533	567	600
Added antennas per range	234	71	57	49	44	40	37	35	33

The central core is 1km across and this can be spanned by nine 111m long antennas. Thus, a covering of the compact core with 234 antennas is achieved with antennas grouped into 26 rows. Each row consist of 9 antennas place end to end giving a total reflector length of 1km. The spacing between the rows is on average 40 m, giving a filling factor (collecting area/physical area) at zenith of 15/40 = .375. If the rows are evenly spaced then shadowing occurs at elevations below 22 degrees. At this elevation the filling factor is 1. The high filling factor of the central core provides the very high surface-brightness sensitivity needed to explore the era of re-ionisation. The trade-off for this is an increased minimum elevation limit. Doubling the area of the compact core would halve the maximum surface-brightness sensitivity and bring the minimum elevation down to 11 degrees. However, it should be noted that for the cylindrical reflector concept at any given minimum elevations the filling factor and hence surface brightness sensitivity is about twice that of parabolic dishes or Luneburg lenses with full mechanical steering.

If different spacings are used between different rows of antennas, as shown in Figure 22, shadowing can be made to occur gradually. Some shadowing will occur at higher elevations but significant collecting area is available at low elevations. This also breaks the regularity of the array and gives better UV coverage. In the case shown, the number of independent UV samples is doubled. However, the minimum spacing between antennas leaves an area of poor UV coverage at small values of V (vacant band across centre).

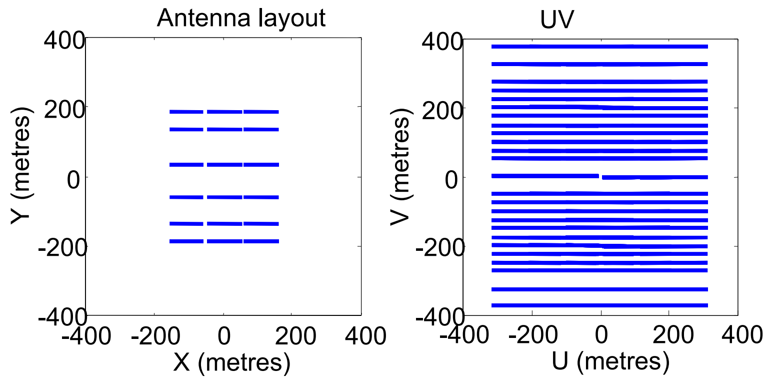

Figure 22 Part of the compact core showing six rows of three antennas. Zenith UV coverage shown right.

These UV values are filled in if the north-south columns of antennas are displaced relative to each other, Figure 22. It is seen that the UV coverage at short baselines is improved and that the gap has been filled.

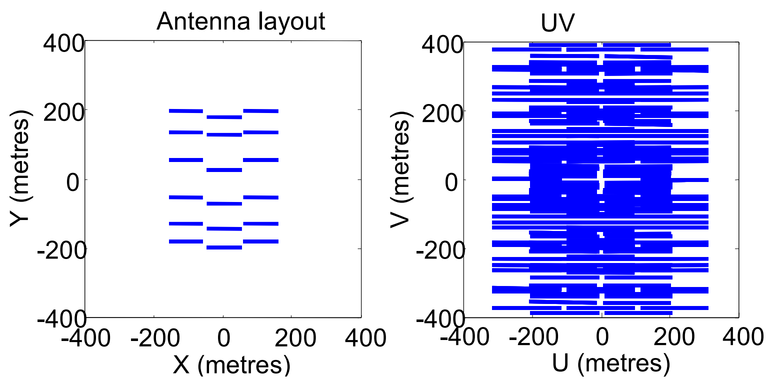

Figure 23 Part of the compact core showing six rows of three antennas with the edge antenna displaced to the north. Zenith UV coverage shown right.

At the next highest maximum baseline, there are 71 antennas (Table 1) that need to be placed within a 39 square kilometre area (the area extends 3.15km from the centre of compact component). There are nearly two antennas per square kilometre. This, together with the fact that each baseline generates two UV samples, means there is a four-fold duplication[6] of the compact component in each square kilometre of zenith UV space. The very abrupt change in fill factor seen at the edge of the compact component can be reduced by increasing the spacing between antennas in the outer part of the compact component or grading the density of the 3.15km antenna. For example, the density of antenna could be eight per square kilometre within 0.5 of the compact core reducing to four in the next kilometre and finally to one per square kilometre in the last 2.15km.

[6] A duplication results from a single antenna being correlated with every antenna in the compact core. In the zenith UV coverage the compact core is replicated with a displacement equal to the distance between the single antenna and the centre of the compact core.

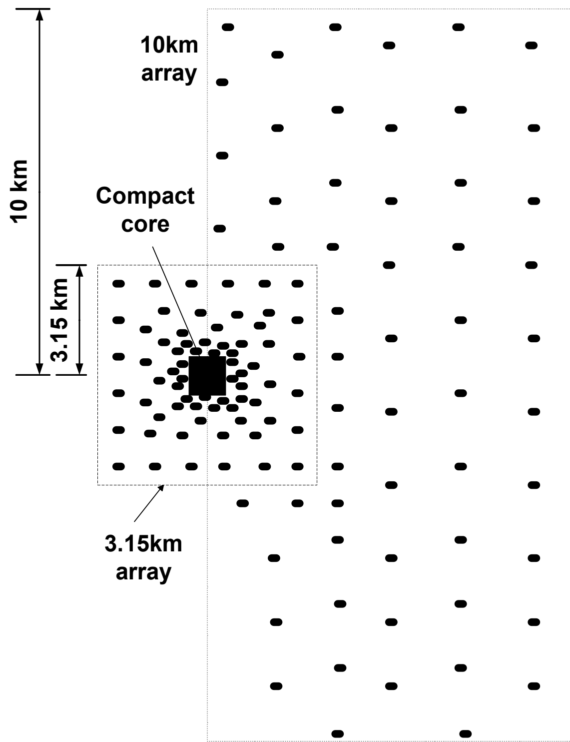

Figure 24 Possible array configuration for baselines 1, 3.15 and 10km

Going from a maximum baseline of 3.15 km to 10 km adds 57 antennas. As only locations to one side to the central core are needed Bunton [1] these are distributed over an area of 190 square km. This provides only one duplication of the compact core every 3.3 square kilometres of UV space. An arrangement as shown in Bunton [1] figure 4b might be used together a small displacement on each column. The area between each duplication of the compact core will be filled with correlation between the 10 and 3.1km antennas, which provide about one-tenth the correlation density available within the duplications of the compact core. A possible arrangement of the antennas for 1, 3.15 and 10km baselines is shown in Figure 24.

At the next maximum baseline, baselines to 31.5 km, there are 49 antennas for 1900 square kilometres, one per 38 square kilometres. The 3.15km antennas cover 40 square kilometres allowing a duplication of the 3.15km antenna array and compact core to fill the UV plane. The density of UV samples at zenith is at least two per square kilometre. Areas of higher sensitivity due to the compact core will occur at regular intervals within this region. Displacement of the rows of antennas will help prevent antennas falling on common radials from the compact core. This allows multi-frequency synthesis to better fill the UV plane. The 31.5km-baseline antennas cover an area of 63 by 31.5km. Suitable sites for a radio quiet reserve of this size have been identified in the Australian states of Western Australia, South Australia, New South Wales and Queensland.

[1] Bunton, J.D., 'Array configurations that tile the plane' Experimental Astrophysics Vol 11, No3 pp193-206, 2001